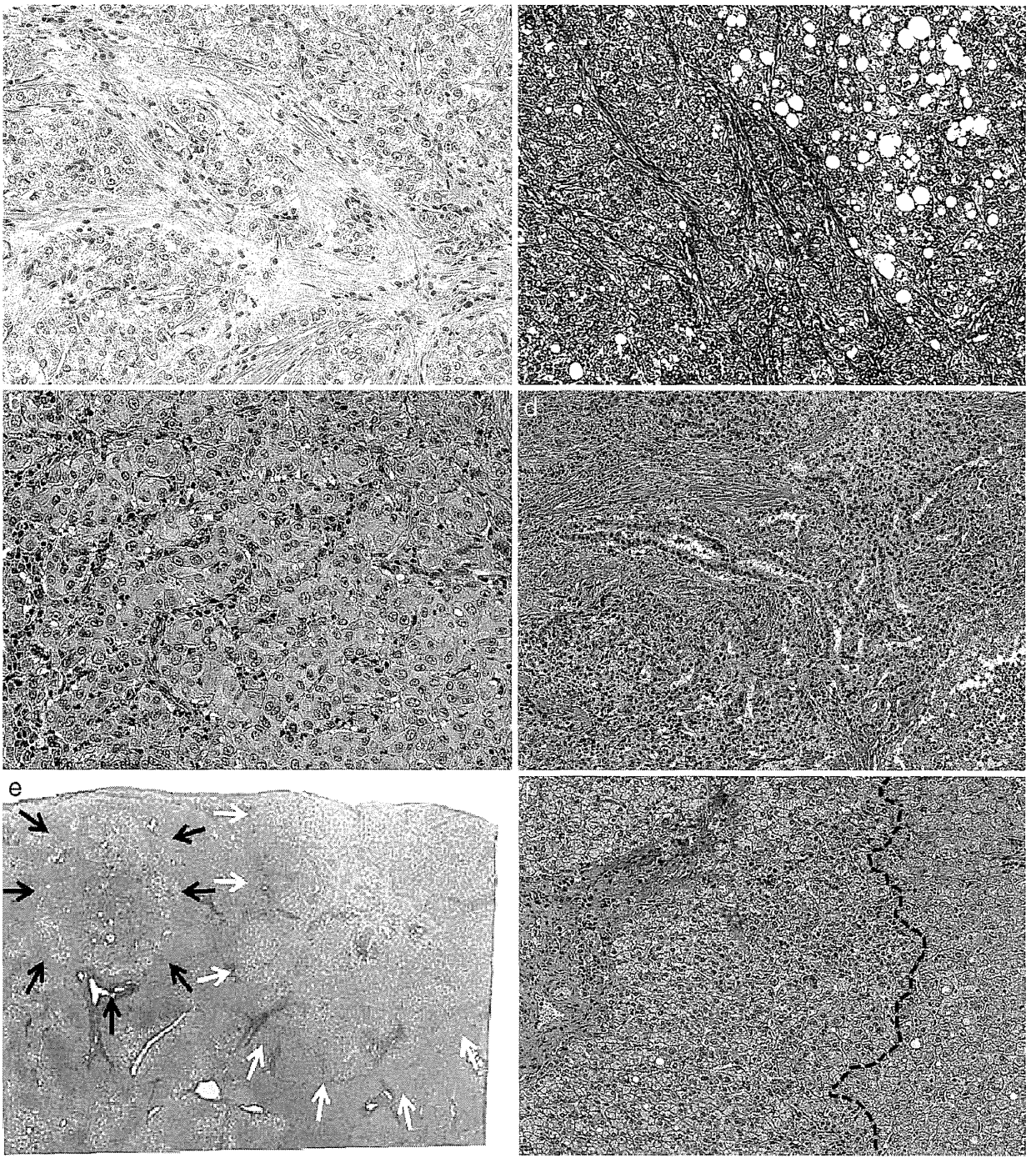

Fig. 3 Microscopic findings. The tumor in S6 was of the scirrhous type of moderately differentiated hepatocellular carcinoma (a) H&E stain (×20) (b) Azan-Mallory stain (×10). S8-A and S8-C lesions were combined HCC-CC. (c) Component of HCC (×20). (d) Component of CCC (×10). S8-B was of the scirrhous type of moderately differentiated hepatocellular carcinoma (indicated by white arrows in loupe observation [e]). S8-D was an early hepatocellular carcinoma (indicated by white arrows in loupe observation [e]). The broken line indicates a borderline between carcinoma in S8-D (left side) and normal area (right side). (f) (×15).

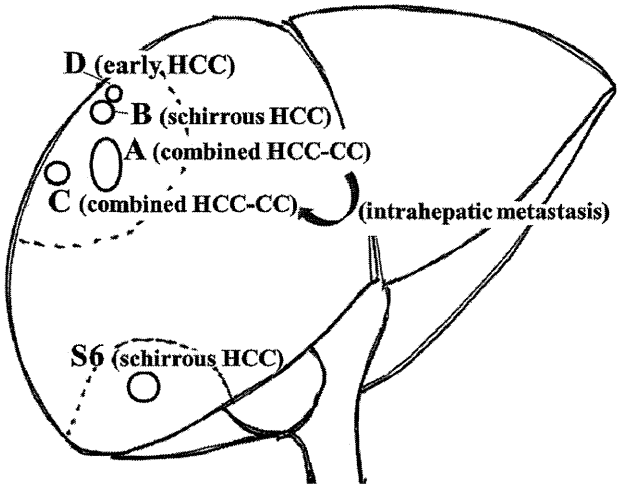

Fig. 4 Locations and pathologic features of 5 hepatic tumors.

In addition, S8-D was thought to be an eHCC. Therefore, we assume that our patient had 5 different coexisting hepatic cancers, of which 4 were primary cancers that arose multicentrically with multiple pathologic features and one was an intrahepatic metastasis.

Scirrhous HCC and combined HCC-CC are rare primary liver cancers, and in Japan, their frequencies have been reported to be approximately 4.6% and 0.54%, respectively, of primary liver cancers.[5,6] Most of the synchronous double primary hepatic cancers are a combination of HCC and CCC, and the frequency of the combination of scirrhous HCC and combined HCC-CC is extremely low. Our patient had 5 tumors, 1 combined HCC tumor with an intrahepatic metastasis, 2 scirrhous HCC-CC tumors, and 1 eHCC tumor. To our knowledge, this is the first published report of the coexistence of 5 hepatic cancers composed of 4 primary cancers with 3 different types of pathologic features in a single patient.

Accuracy and feasibility of preoperative diagnosis for primary hepatic cancers are of great interest. In our patient, 3 tumors (S6, S8-A, and S8-B) were preoperatively identified by CT and MRI, but 2 tumors (S8-C, 6 mm and S8-D, 4 mm) could not be identified, even by the retrospective assessment of the preoperative CT and MRI data. It is sometimes difficult to detect such tiny tumors using the currently available diagnostic devices. With regard to the 3 identified tumors, the preoperative diagnoses were not correct. The S6 and S8-B tumors were preoperatively diagnosed as classic HCC, but were in fact histologically a rare variant of HCC, scirrhous HCC. One of the characteristic features of scirrhous HCC is prolonged enhancement in the late phase in CT and MRI imaging,[7] but the feature varies depending on individual tumors. In addition, the finding of prolonged enhancement in the late phase is not specific to scirrhous HCC, and is frequently seen in CCC and metastatic tumors. Therefore, it is usually difficult to preoperatively diagnose scirrhous HCC. The preoperative CT findings of these 2 tumors showed early enhancement and washout (or isodensity) and were not consistent with the typical features or any features that are strongly associated with scirrhous HCC, suggesting that they were typical HCCs. We have to be aware that tumors with features that closely resemble the typical findings of HCC could also be differentially diagnosed as a rare variant of scirrhous HCC. The S8-A tumor was in fact histologically combined HCC-CC. The diagnosis of CCC or combined HCC-CC requires extra attention because additional operative procedures, such as lymph node dissection, may be necessary. However, definitive preoperative diagnosis of combined HCC-CC, in particular, seems to be challenging.[8] In our patient, although combined HCC-CC was included in the preoperative differential diagnosis of the S8-A tumor based on CT and MRI findings, we could not pinpoint the diagnosis to combined HCC-CC before surgery. Nakamura *et al*[9] hypothesized that a hypervascular tumor with high CEA and CA19-9 levels or a hypovascular tumor with a high level of AFP may indicate a preoperative diagnosis of combined HCC-CC, but these features did not correspond to our patient. Further advances in diagnostic devices or markers are needed to differentiate relatively rare hepatic cancers, such

as scirrhous HCC and combined HCC-CC, from typical HCCs.

Surgical intervention is another point of interest for primary hepatic cancers with multiple pathologic features, especially if CCC or combined HCC-CC is involved. The necessity of hilar lymph node dissection for combined HCC-CC is still under debate.[9,10] At our institute, hilar lymph node dissection is performed for preoperatively diagnosed combined HCC-CC in cases where the hilar lymph nodes appear metastatic from the preoperative imaging diagnosis or observation during surgery. In our patient, because the lymph nodes were not preoperatively and intraoperatively suspected to be metastatic, lymph node dissection was not performed. Postsurgical care, such as additional treatments including lymph node dissection or adjuvant chemotherapy, could be necessary in the future considering the possible recurrence in lymph nodes from the combined HCC-CC tumors in S8-A and S-8C. We have no immediate plans to do so because postoperative CT and serum tumor markers have not indicated any signs of recurrence at present, and we need to consider that the appearance of another tumor may not be lymph node metastasis but instead may be a multicentric occurrence of a new HCC. Considering the pathologic features of this patient, the possibility of a new HCC occurrence in the future is high. We will continue examining this patient by CT and tumor markers every 6 months so we can immediately plan the appropriate treatments for any recurrence such as lymph node metastasis or new HCC.

We reported a very rare case of 5 different coexisting hepatic cancers, whose pathologic features included scirrhous HCC and combined HCC-CC. Because of rarity and the diseases' natural characters, definite preoperative diagnoses were difficult in this patient. Special attention should always be given when encountering patients in whom unexpected tumors or whose tumor features are different from the preoperative diagnosis. The postoperative course of this patient is pathophysiologically interesting because the multiple pathologic features could have various patterns of recurrence. Considering the pathophysiologic characters of each tumor, long-term observation of the patient is necessary.

References

1. Liver Cancer Study Group of Japan. Survey and follow-up study of primary liver cancer in Japan. Report 13. *Acta Hepatol Jpn* 1999;**40**(5):288–300
2. Takano S, Yokosuka O, Imazeki F, Tagawa M, Omata M. Incidence of hepatocellular carcinoma in chronic hepatitis B and C: a prospective study of 251 patients. *Hepatology* 1995;**21**(3):650–655
3. Simonetti RG, Camma C, Fiorello F, Cottone M, Rapicetta M, Marino L *et al.* Hepatitis C virus infection as a risk factor for hepatocellular carcinoma in patients with cirrhosis. A case-control study. *Ann Intern Med* 1992;**116**(2):97–102
4. De Mitri MS, Poussin K, Baccarini P, Pontisso P, D'Errico A, Simon N *et al.* HCV-associated liver cancer without cirrhosis. *Lancet* 1995;**345**(8947):413–415
5. Kurogi M, Nakashima O, Miyaaki H, Fujimoto M, Kojiro M. Clinicopathological study of scirrhous hepatocellular carcinoma. *J Gastroenterol Hepatol* 2006;**21**(9):1470–1477
6. Ikai I, Itai Y, Okita K, Omata M, Kojiro M, Kobayashi K *et al.* Report of the 15th follow-up survey of primary liver cancer. *Hepatol Res* 2004;**28**(1):21–29
7. Kim SR, Imoto S, Nakajima T, Ando K, Mita K, Fukuda K *et al.* Scirrhous hepatocellular carcinoma displaying atypical findings on imaging studies. *World J Gastroenterol* 2009;**15**(18): 2296–2299
8. Taguchi J, Nakashima O, Tanaka M, Hisaka T, Takazawa T, Kojiro M A. Clinicopathological study on combined hepatocellular and cholangiocarcinoma. *J Gastroenterol Hepatol* 1996;**11**(8):758–764
9. Nakamura S, Suzuki S, Sakaguchi T, Serizawa A, Konno H, Baba S *et al.* Surgical treatment of patients with mixed hepatocellular carcinoma and cholangiocarcinoma. *Cancer* 1996;**78**(8):1671–1676
10. Sasaki A, Kawano K, Aramaki M, Ohno T, Tahara K, Takeuchi Y *et al.* Clinicopathologic study of mixed hepatocellular and cholangiocellular carcinoma: modes of spreading and choice of surgical treatment by reference to macroscopic type. *J Surg Oncol* 2001;**76**(1):37–46

Clin J Gastroenterol (2012) 5:189–194
DOI 10.1007/s12328-012-0296-3

CASE REPORT

Hemobilia due to biliary intraepithelial neoplasia associated with Zollinger–Ellison syndrome

Rumiko Umeda · Yuji Nakamura · Yohei Masugi · Masahiro Shinoda · Naoki Hosoe · Yoshihiro Ono · Tomonori Fujimura · Yoshiyuki Yamagishi · Hajime Higuchi · Hirotoshi Ebinuma · Shigenari Hozawa · Minoru Tanabe · Subaru Hashimoto · Michiie Sakamoto · Yuko Kitagawa · Toshifumi Hibi

Received: 30 January 2012 / Accepted: 21 March 2012 / Published online: 21 April 2012

Abstract A 58-year-old man was transferred to us from his local hospital because of failure to control his gastrointestinal bleeding by endoscopic hemostasis. Abdominal imaging suggested a hypervascular tumor of the pancreatic head (36 mm diameter), and laboratory testing showed an elevated serum gastrin level (17,800 pg/mL). Gastroduodenal endoscopy revealed multiple duodenal ulcers and active bleeding from the ampulla of Vater. The selective arterial secretagogue injection test suggested a gastrinoma in the pancreatic head, but no gastrinoma in the pancreatic tail. The patient was diagnosed with solitary pancreatic head gastrinoma complicated by hemosuccus pancreaticus, and pancreaticoduodenectomy was performed. Intraoperatively, the diagnosis was changed to primary peripancreatic lymph node gastrinoma without pancreatic involvement. The gastrointestinal bleeding stopped postoperatively and serum gastrin levels returned to normal. Histological examination of the surgical specimens revealed a small submucosal gastrinoma in the duodenum (7 mm diameter). The final diagnosis was microgastrinoma of the duodenum with peripancreatic lymph node metastasis. The cause of bleeding from the ampulla of Vater was initially obscure, but eventually a hemorrhagic erosion with moderate atypia was found in the common bile duct, indicating biliary intraepithelial neoplasia (BilIN). This is the first report of hemobilia due to BilIN with gastrinoma.

Keywords Biliary intraepithelial neoplasia · Hemobilia · Gastrinoma · Zollinger–Ellison syndrome · GI bleeding

R. Umeda · Y. Nakamura (✉) · N. Hosoe · Y. Yamagishi · H. Higuchi · H. Ebinuma · S. Hozawa · T. Hibi
Division of Gastroenterology and Hepatology, Department of Internal Medicine, School of Medicine, Keio University, 35 Shinanomachi, Shinjuku, Tokyo 160-8582, Japan
e-mail: yujinaka@a5.keio.jp

R. Umeda
e-mail: rumiko0124@z5.keio.jp

Y. Masugi · M. Sakamoto
Department of Pathology, School of Medicine, Keio University, Tokyo, Japan

M. Shinoda · Y. Ono · T. Fujimura · M. Tanabe · Y. Kitagawa
Department of Surgery, School of Medicine, Keio University, Tokyo, Japan

S. Hashimoto
Department of Diagnostic Radiology, School of Medicine, Keio University, Tokyo, Japan

Introduction

Zollinger–Ellison syndrome (ZES) was first described in 1955 by Robert Zollinger and Edwin Ellison, surgeons at Ohio State University, USA. This syndrome presents with a triad of acid hypersecretion, severe peptic ulceration, and gastrinoma (non-beta islet cell tumor of the pancreas that secretes large amounts of gastrin) [1]. ZES is rare, with an incidence of about 1 case per million people per year in the USA. Solitary lesions are located in the duodenum in 50–70 % of cases and in the pancreas in 20–40 % of cases. More than 90 % of gastrinomas are found in the anatomical triangle referred to as the gastrinoma triangle, which has vertices at (a) the confluence of the cystic and common bile ducts, (b) the junction of the second and third portions of the duodenum, and (c) the junction of the neck and body of the pancreas [2]. Duodenal gastrinomas are usually much smaller than pancreatic gastrinomas. When the primary lesion is not located in either the pancreas or the duodenum, primary lymph node gastrinoma is diagnosed.

In 2005, Zen et al. [3] proposed 3 grades of biliary intraepithelial neoplasia (BilIN) after analyzing atypical/proliferative lesions of the intrahepatic bile ducts in patients with hepatolithiasis. BilIN occurs in cases of cholelithiasis, familial adenomatous polyposis, sclerosing cholangitis, and pancreatobiliary reflux, and is categorized into 3 types (BilIN-1, low-grade; BilIN-2, intermediate-grade; and BilIN-3, high-grade/carcinoma in situ) [4]. BilIN is characterized by atypical epithelial cells with multilayering of nuclei and micropapillary projections into the lumen, and is believed to play a major role in the development of cholangiocarcinoma through a dysplasia-to-carcinoma sequence. Expression of TP53 is helpful in identifying dysplastic changes, which are more common and extensive in BilIN than in reactive epithelium.

Bleeding from the ampulla of Vater is a rare type of gastrointestinal (GI) bleeding, and can be caused by diseases of the ampulla of Vater, the pancreatic duct, or the biliary duct. Hemosuccus pancreaticus is bleeding from the pancreatic duct, pancreas, and structures adjacent to the pancreas. Hemobilia is a manifestation of hepatobiliary disease, and is most commonly caused by medical interventions such as liver surgery or by blunt abdominal trauma, and less commonly by hepatobiliary diseases such as hepatic artery aneurysm or biliary tract neoplasm. Here we report a case of ZES with active bleeding from the ampulla of Vater, which was initially diagnosed as hemosuccus pancreaticus due to pancreatic gastrinoma. After surgical resection of the structures in the gastrinoma triangle, histological examination of the resected specimens revealed microgastrinoma of the duodenum with metastasis to a peripancreatic lymph node, and a hemorrhagic erosion in the common bile duct with atypical epithelial cells indicating BilIN. Although several cases of hemobilia due to carcinoma have been reported [5, 6], this is the first report of hemobilia due to BilIN in a patient with ZES.

Case report

A 58-year-old man was transferred from his local hospital to our hospital with uncontrolled GI bleeding from multiple duodenal ulcers. He had visited his local hospital complaining of melena and faintness 10 days previously, and gastroduodenal endoscopy had revealed active bleeding from duodenal ulcers. Although he underwent two sessions to achieve endoscopic hemostasis with hemoclipping and ethanol injection, the GI bleeding continued and he required multiple blood transfusions. He had a history of watery diarrhea of undetermined cause for one year. The laboratory data obtained at our hospital are shown in Table 1. Abdominal ultrasonography (US), computed tomography (CT), and magnetic resonance imaging (MRI) showed a hypervascular mass measuring 36 × 28 mm (Fig. 1), which was reported to be suggestive of a neuroendocrine tumor in the pancreatic head. As serum gastrin level was elevated (17800 pg/mL), ZES was diagnosed. Gastroduodenal endoscopic examination revealed multiple duodenal ulcer scars, and hemoclips which had been placed at his local hospital. No active bleeding was observed from the duodenal mucosa, but fresh bleeding was observed from the ampulla of Vater (Fig. 2). We diagnosed hemosuccus pancreaticus due to pancreatic gastrinoma and explained to the patient that treatment would require resection. To determine the operability and location of the gastrinoma, angiography and the selective arterial secretagogue injection (SASI) test were performed. The SASI

Table 1 Laboratory data obtained on admission to our hospital

WBC	6,500/mL	TP	3.9 g/dL	Glu	132 mg/dL
Seg	82 %	Alb	2.2 g/dL	TG	129 mg/dL
Lymph	15 %	TB	0.3 mg/dL	HDL-C	24 mg/dL
Mono	3 %	BUN	16.1 mg/dL	LDL-C	69 mg/dL
RBC	283 × 10^4/mL	Crtnn	1.06 mg/dL	AMY	88 IU/L
Hb	8.6 g/dL	UA	7.9 mg/dL	CRP	0.02 mg/dL
Hct	27.3 %	Na	139 mEq/L	Fe	114 μg/dL
Plt	40 × 10^4/mL	K	4.3 mEq/L	TIBC	339 μg/dL
APTT	26.6 s	Cl	108 mEq/L	PTH-intact	45 pg/mL
PT	10.2 s	Ca	7.4 mg/dL	Calcitonin	30 pg/mL
PT-INR	0.97	IP	2.7 mg/dL	IRI	11 μU/mL
FNG	275 mg/dL	AST	18 IU/L	C-peptide	5.5 ng/mL
		ALT	26 IU/L	Gastrin	17,800 pg/mL
		LDH	150 IU/L		
		ALP	143 IU/L		
		γ-GTP	14 IU/L		

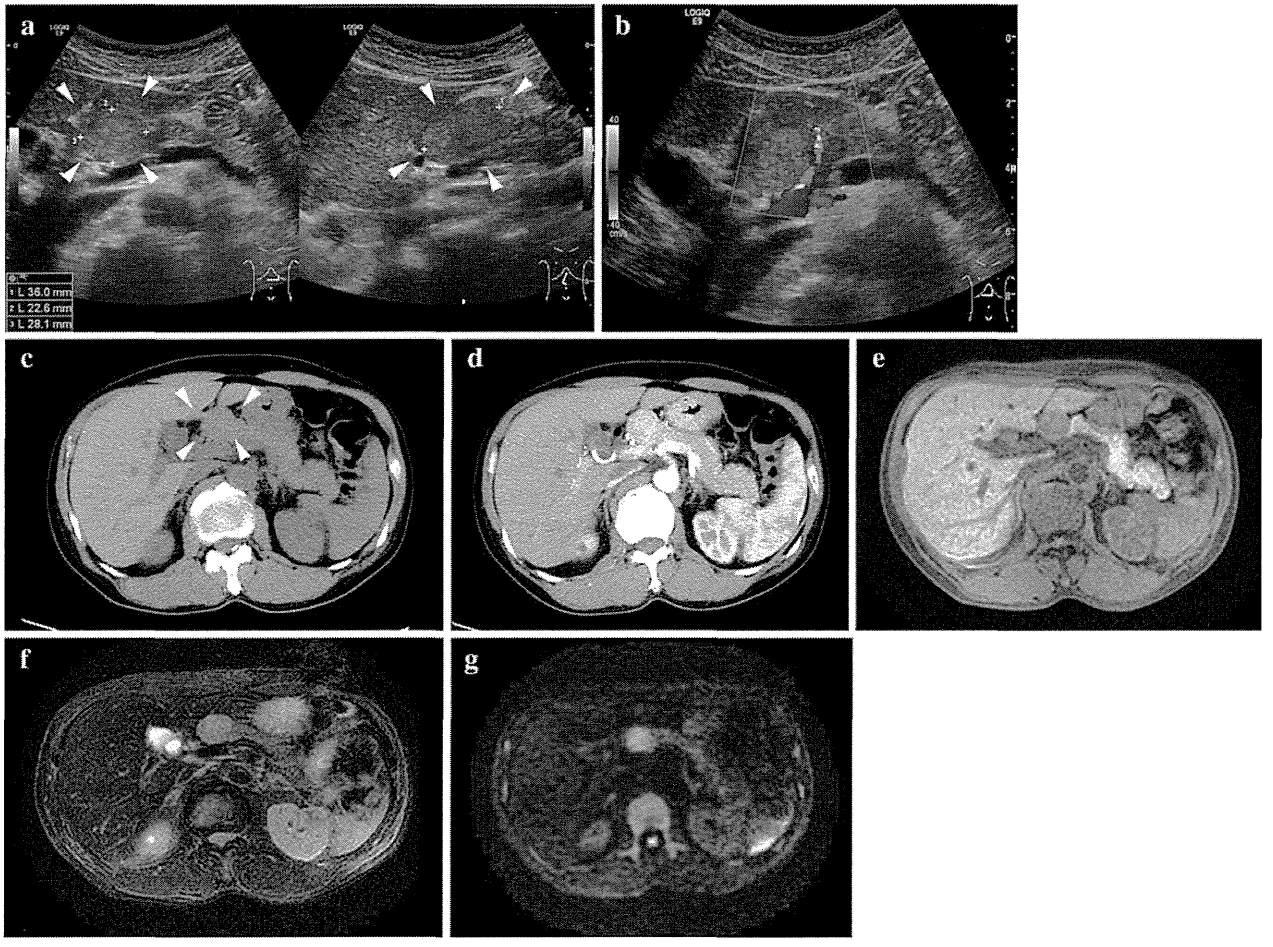

Fig. 1 Abdominal images. **a** Ultrasonography showed a hyperechoic tumor (36 × 28 mm) in the pancreatic head. **b** Doppler imaging showed a vascular signal in the mass. **c** Computed tomography showed an isodense tumor in the pancreatic head. **d** Contrast enhancement showed the vascularity of the tumor. **e** T1-weighted magnetic resonance imaging (MRI) showed a low-intensity tumor. **f** T2-weighted MRI showed a high-intensity tumor. **g** Diffusion-weighted MRI showed a high-intensity tumor. The *arrowheads* indicate the tumor

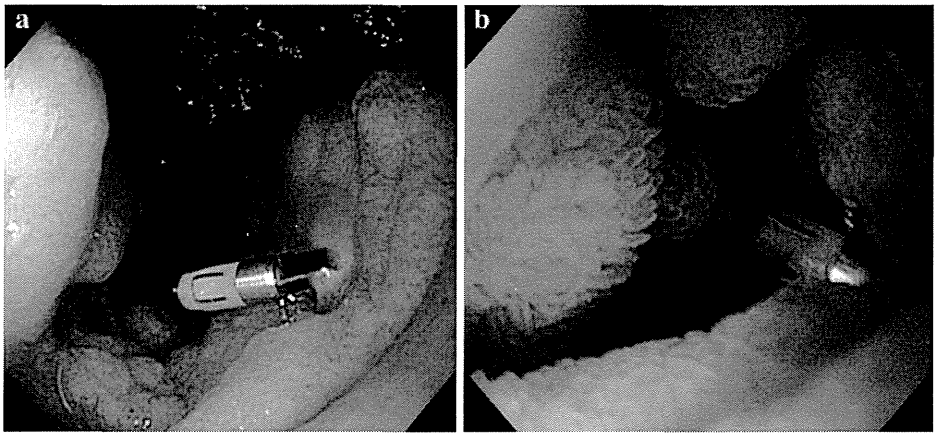

Fig. 2 Images obtained by gastroduodenal endoscopy. **a** The hemoclip which was attached to the second portion of the duodenum opposite the ampulla of Vater at the patient's local hospital. **b** Active bleeding from the ampulla of Vater

test gave positive results for celiac, superior mesenteric, and inferior pancreaticoduodenal artery injection, but negative results for splenic and transverse pancreatic artery injection (Table 2), indicating gastrinoma in the pancreatic head but not in the pancreatic tail. Pancreaticoduodenectomy was performed.

Table 2 Selective arterial secretagogue injection test (SASI) results

	0 s	30 s	60 s	90 s	120 s	180 s
CA	8,650	27,800	16,000	14,700	12,000	14,700
SMA	9,150	46,400	27,000	22,000	20,600	21,200
IPDA	10,800	61,500	31,700	26,300	26,300	18,000
TPA	9,100	8,810	10,100	12,100	95,300	11,700
SA	14,000	13,200	12,800	16,100	14,700	13,300

Blood samples were taken from the hepatic vein at 0, 30, 60, 90, 120, and 180 s after injection of calcium solution (1 mEq), and gastrin levels were measured (pg/mL)

CA celiac artery, *SMA* superior mesenteric artery, *IPDA* inferior pancreaticoduodenal artery, *TPA* transverse pancreatic artery, *SA* splenic artery

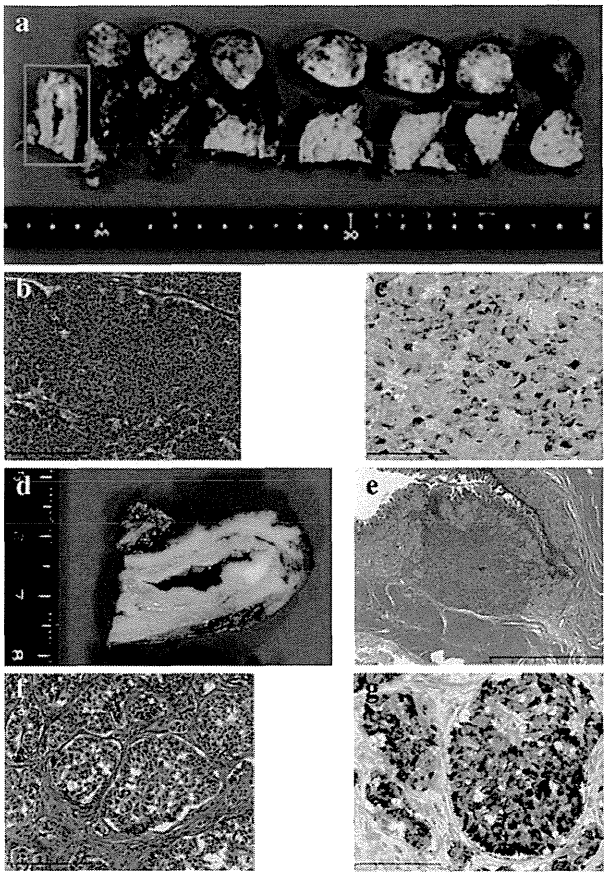

Fig. 3 Surgically excised tissues. **a** Macroscopic appearance of the excised peripancreatic tumor and the head of the pancreas. The duodenal tumor is shown in the rectangle at the *left*. **b** Microscopic appearance of the peripancreatic tumor stained with hematoxylin and eosin (H&E) (×20), showing that the tumor was a lymph node metastasis. **c** The metastatic lymph node showed positive staining for gastrin (×20). **d** Macroscopic appearance of the submucosal microtumor in the second portion of the duodenum. **e** Loupe image of the submucosal microtumor in the second portion of the duodenum. **f** Microscopic appearance of the tumor in the second portion of the duodenum stained with H&E (×20). **g** The tumor in the second portion of the duodenum showed positive staining for gastrin

Pathological examination of the excised tissues revealed that the gastrinoma was not located in the pancreas, but in a lymph node measuring 30 × 28 × 23 mm near the common hepatic artery at the head of the pancreas (Fig. 3). A small submucosal tumor (7 mm diameter) was found in the second portion of the duodenum. Immunohistochemical studies for gastrin showed the same pattern of positive staining in the duodenal tumor and in the affected lymph node. The final diagnosis was duodenal microgastrinoma with metastasis to a peripancreatic lymph node. The mitotic count was 3 per 10 high-power fields and the Ki67 index was 2–3 %, giving a World Health Organization classification of NET G2. Postoperative review of the CT, MRI, and US scans indicated that the mass detected on preoperative images was compatible with a peripancreatic tumor. Review of the angiography and SASI test results could not distinguish between pancreatic and peripancreatic tumor.

No bleeding lesions were observed in the pancreas or the ampulla of Vater, but a hemorrhagic erosion was detected in the bile duct, associated with atypical biliary epithelial cells with multilayering of nuclei and micropapillary projections into the lumen. There was an abrupt transition between the area of cellular abnormalities and the normal biliary epithelium, indicating BilIN rather than reactive changes (Fig. 4). Immunohistochemical analysis demonstrated strongly positive immunolabeling for Ki-67 and positive staining for TP53. No stromal invasion or severe atypia regarded as carcinoma was observed. The pathological change in the bile duct was diagnosed as BilIN-2/3 with hemorrhagic erosion. The gastrin level decreased back to normal postoperatively (39 pg/mL), and the patient's anemia resolved without further need for blood transfusion.

Discussion

To the best of our knowledge, this is the first report of hemobilia due to BilIN in a patient with ZES. The clinical features of hemobilia include upper abdominal pain, upper GI hemorrhage, and jaundice, and all three may be present in up to 22 % of cases [7]. Hemobilia is most commonly reported when there is a history of liver injury or

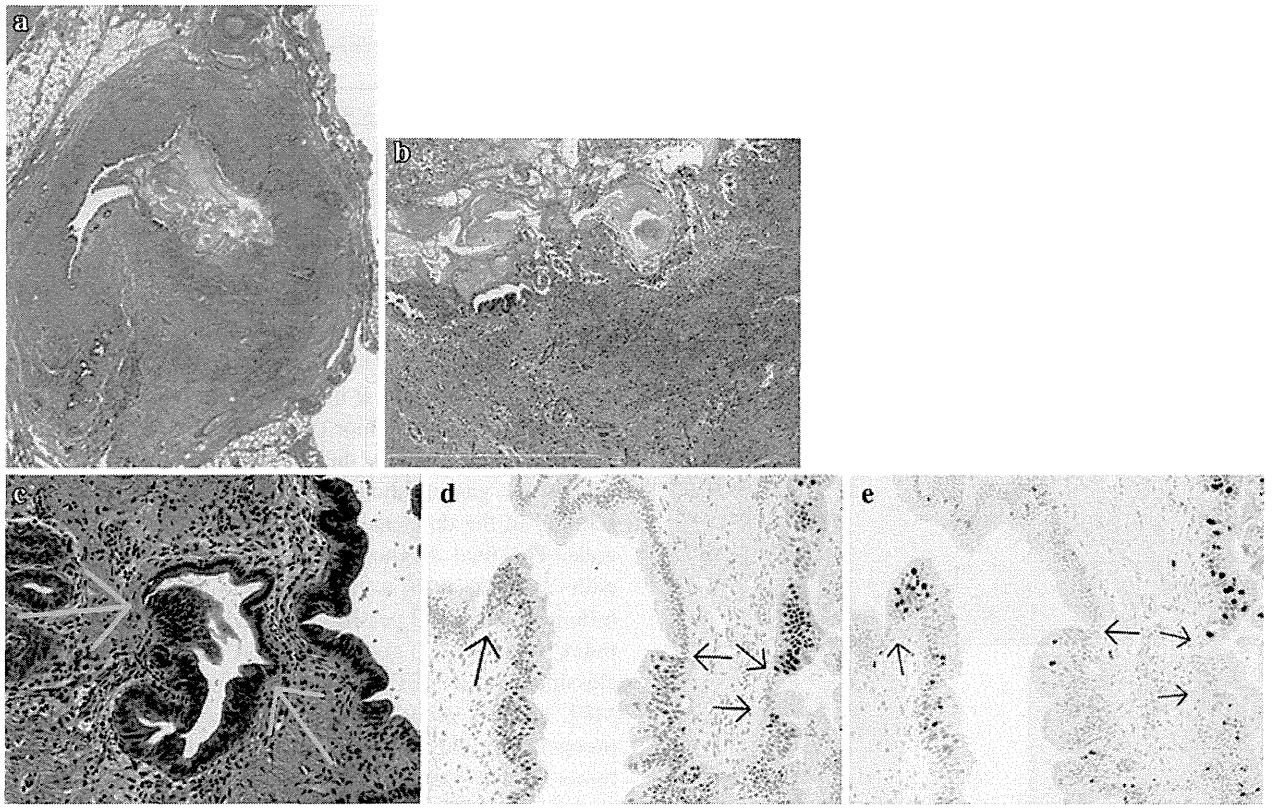

Fig. 4 **a** Loupe image of the hemorrhagic erosion in the bile duct. **b** Microscopic appearance of the hemorrhagic erosion in the bile duct (H&E staining, ×10). **c** Dysplastic biliary epithelial cells with multilayering of nuclei and micropapillary projections into the lumen (×10). The *green arrows* indicate an abrupt transition between the dysplastic and normal epithelial cells. **d**, **e** Immunostaining of serial sections for TP53 and Ki-67. The *black arrows* indicate the borders between the dysplastic and normal epithelial cells (×20)

instrumentation, such as percutaneous biliary drainage (19 % of cases), liver biopsy (13 %), or cholecystectomy (13 %). Cholangiocarcinoma is not a major cause of hemobilia and is present in only 3 % of cases. The present case had GI bleeding but no abdominal pain or jaundice. The duodenal ulceration due to ZES initially masked the hemorrhage from the biliary tract, and bleeding from the ampulla of Vater was found during endoscopic examination for recurrent duodenal ulcer bleeding.

In our patient, the initial impression was of a solitary gastrinoma in the pancreatic head with hemorrhage at the ampulla of Vater. The preoperative diagnosis was therefore hemosuccus pancreaticus due to a hypervascular gastrinoma of the pancreas. We did not perform endoscopic retrograde cholangiopancreatography or endoscopic US, because repeated blood transfusions were required to treat the anemia and it was necessary to operate as soon as possible. The multiple duodenal ulcers which had required hemoclipping also increased the risk of rebleeding during endoscopic US. However, the postoperative diagnosis was microgastrinoma of the duodenum with peripancreatic lymph node metastasis but no pancreatic invasion. Conventional imaging studies fail to identify the exact location of 80 % of microgastrinomas of the duodenum because of their small size. Postoperative review of the duodenoscopy images did not detect the primary lesion. Primary lymph node gastrinomas are not particularly rare, accounting for approximately 10 % of sporadic cases [8]. Somatostatin receptor scintigraphy (SRS), a procedure commonly used to detect duodenal gastrinomas in other countries but not currently approved for use by the Japanese Ministry of Health, Labour and Welfare, is reportedly helpful in detecting occult primary gastrinomas >10 mm in diameter. As the tumor in this case was only 7 mm it might not have been detectable by SRS. Hepatic metastasis is the most important predictor of poor survival, because the lymph nodes in the gastrinoma triangle can be removed with a standard pancreaticoduodenectomy [9]. As there were no hepatic lesions in this case, no additional therapy was given.

In our case, BilIN was associated with gastrinoma. Gastrin directly stimulates the parietal cells of the stomach to secrete hydrochloric acid, and also indirectly stimulates hydrochloric acid secretion by binding to the cholecystokinin-B receptors on the enterochromaffin cells in the stomach, thereby causing histamine release which

stimulates the parietal cells. Gastrin has also been shown to have additional functions such as stimulating pancreatic secretion and gallbladder emptying [10]. However, there are no published reports describing a relationship between gastrinoma and bile duct neoplasia. Further studies are needed to evaluate the potential biliary stress caused by gastrin oversecretion. In this case, we found an erosive hemorrhagic lesion with dysplasia in the bile duct. As BilIN is limited to the mucosal layer, it seems unlikely that it would cause bleeding. Although we tried to find a relationship between the BilIN lesion and the source of bleeding histopathologically, we were unable to find one from the excised tissues. However, there have been several reports of other mucosal lesions causing bleeding, such as gastric hyperplastic polyp [11], colon adenoma [12], and bladder dysplasia [13]. Expression of TP53 has been reported to be low in early BilIN and significantly increased in invasive cholangiocarcinoma [14]. The relatively high positivity for TP53 staining in this case is highly suspicious of a carcinomatous lesion.

In conclusion, we experienced a rare case of hemobilia due to BilIN associated with ZES, which was difficult to diagnose. Surgery for gastrinoma must include complete resection of the gastrinoma triangle by pancreaticoduodenectomy, and hemobilia associated with a bile duct neoplasm should be considered as a cause of GI bleeding that is difficult to control.

Conflict of interest The authors declare that they have no conflict of interest.

References

1. Jensen RT. Gastrinoma. In: Holzheimer RG, Mannick JA, editors. Surgical treatment. Evidence-based and problem-oriented. Munich: Zuckschwerdt; 2001.
2. Fendrich V, Langer P, Waldmann J, Bartsch DK, Rothmund M. Management of sporadic and multiple endocrine neoplasia type 1 gastrinomas. Br J Surg. 2007;94:1331–41.
3. Zen Y, Aishima S, Ajioka Y, Kage M, Kondo F, Nimura Y, et al. Proposal of histological criteria for intraepithelial atypical/proliferative biliary epithelial lesions of the bile duct in hepatolithiasis with respect to cholangiocarcinoma: preliminary report based on interobserver agreement. Pathol Int. 2005;55:180–8.
4. Bosman FT, Carneiro F, Hruban RH, Theise ND. Biliary intraepithelial neoplasia. In: WHO classification of tumors of the digestive system, 4th ed. WHO, Washington DC; 2010. p. 270.
5. Alapati R, Ibrahim MA, D'Angelo DM, Malhotra SK, Nensey YM, Salah-Eldin AA, et al. Papillary cystadenocarcinoma of the bile ducts resulting in hemobilia. Am J Gastroenterol. 1989;84:1564–6.
6. Pasos-Altamirano G, Mendieta-Zeron H, Fuentes-Luiton E. Hemobilia. A case report. Ann Hepatol. 2003;2:141–2.
7. Green MHA, Duell RM, Johnson CD, Jamieson NV. Haemobilia. Br J Surg. 2001;88:773–86.
8. Norton JA, Alexander HR, Fraker DL, Venzon DJ, Gibril F, Jensen RT. Possible primary lymph node gastrinoma: occurrence, natural history, and predictive factors: a prospective study. Ann Surg. 2003;237:650–7.
9. Norton JA. Surgical treatment and prognosis of gastrinoma. Best Pract Res Clin Gastroenterol. 2005;19:799–805.
10. Valenzuela JE, Walsh JH, Isenberg JI. Effect of gastrin on pancreatic enzyme secretion and gallbladder emptying in man. Gastroenterology. 1976;71:409–11.
11. Jain R, Chetty R. Gastric hyperplastic polyps: a review. Dig Dis Sci. 2009;54:1839–46.
12. Ciatto S, Martinelli F, Castiglione G, Mantellini P, Rubeca T, Grazzini G, Bonanomi AG, Confortini M, Zappa M. Association of FOBT-assessed faecal Hb content with colonic lesions detected in the Florence screening programme. Br J Cancer. 2011;104:1779–85.
13. Cheng L, Cheville JC, Neumann RM, Bostwick DG. Natural history of urothelial dysplasia of the bladder. Am J Surg Pathol. 1999;23:443–7.
14. Nakanishi Y, Zen Y, Kondo S, Itoh T, Itatsu K, Nakanuma Y. Expression of cell cycle-related molecules in biliary premalignant lesions: biliary intraepithelial neoplasia and biliary intraductal papillary neoplasm. Hum Pathol. 2008;39:1153–61.

Cancer Science
The official journal of the Japanese Cancer Association JCA

Direct inhibition of the transforming growth factor-β pathway by protein-bound polysaccharide through inactivation of Smad2 signaling

Yoshihiro Ono,[1] Tetsu Hayashida,[1,3] Ayano Konagai,[1] Hiroshi Okazaki,[1] Kazuhiro Miyao,[1] Shigeyuki Kawachi,[1] Minoru Tanabe,[1] Masahiro Shinoda,[1] Hiromitsu Jinno,[1] Hirotoshi Hasegawa,[1] Masaki Kitajima[2] and Yuko Kitagawa[1]

[1]Department of Surgery, Keio University School of Medicine, Tokyo; [2]International University of Health and Welfare, Tochigi, Japan

(Received June 11, 2011/Revised October 19, 2011/Accepted October 20, 2011/Accepted manuscript online October 29, 2011/Article first published online November 28, 2011)

Transforming growth factor-β (TGF-β) is involved in the regulation of cell proliferation, differentiation, and apoptosis and is associated with epithelial–mesenchymal transition (EMT). Inhibition of the TGF-β pathway is an attractive strategy for the treatment of cancer. We recently screened for novel TGF-β inhibitors among commercially available drugs and identified protein-bound polysaccharide (PSK) as a strong inhibitor of the TGF-β-induced reporter activity of 3TP-lux, a TGF-β1-responsive luciferase reporter. Protein-bound polysaccharide is used as a non-specific immunostimulant for the treatment of gastric and colorectal cancers in Japan. The anticancer activity of this agent may involve direct regulation of growth factor production and enzyme activity in tumors in addition to its immunomodulatory effect. Although several clinical studies have shown the beneficial therapeutic effects of PSK on various types of tumors, its mechanism of action is not clear. In the present study, Western blot analysis showed that PSK suppressed the phosphorylation and nuclear localization of the Smad2 protein, thereby suggesting that PSK inhibits the Smad and MAPK pathways. Quantitative PCR analysis showed that PSK decreased the expression of several TGF-β pathway target genes. E-cadherin and vimentin immunohistochemistry showed that PSK suppressed TGF-β1-induced EMT, and FACS analysis showed that PSK inhibited the EMT-mediated generation of $CD44^+/CD24^-$ cells. These data provide new insights into the mechanisms mediating the TGF-β-inhibiting activity of PSK and suggest that PSK can effectively treat diseases associated with TGF-β signaling. (*Cancer Sci* 2012; 103: 317–324)

Transforming growth factor-β (TGF-β) is involved in various biological activities, such as cell proliferation, differentiation, and apoptosis[1–3] and is also considered a major inducer of epithelial–mesenchymal transition (EMT) during development.[4,5] Inactivation of the TGF-β pathway during the early stages of carcinoma may contribute to carcinogenesis because TGF-β signaling is implicated in the negative regulation of cell proliferation.[2,6] Paradoxically, TGF-β is often overexpressed in malignant cells and alters tumor-specific cell fates and facilitates immunosuppression, deposition of ECM proteins, and angiogenesis.[7,8] Cancer cells overexpressing active TGF-β1 showed increased metastatic ability,[9] and targeting of TGF-β signaling prevented metastasis in several neoplastic tumors including breast, prostate, and colorectal cancers.[10,11] Furthermore, recent studies have suggested new roles for TGF-β signaling in the tumor microenvironment associated with the regulation of cancer stem cells and their niches.[12,13] Clinical studies have shown a positive correlation between TGF-β1 expression and metastasis and poor prognosis in gastric, breast, and colorectal carcinomas.[14–18] Thus, the inhibition of invasion and metastasis through inhibition of the TGF-β pathway could be a promising treatment strategy. However, the application of inhibitors in standard cancer therapy requires both careful evaluation of the clinical benefits and the development of effective strategies to overcome the side-effects associated with the toxicity of these agents.

A previous study suggested that protein-bound polysaccharide (PSK) modulates the biological activity of TGF-β1 and β2 by binding to their active forms.[19] Protein-bound polysaccharide obtained from *Basidiomycetes* has been used as an agent in the treatment of cancer in Asia for over 30 years.[20,21] The anticancer activity of PSK, which is derived from the fungus *Coriolus versicolor*, has been documented in experimental models *in vitro*[22] and in human clinical trials. Several randomized clinical trials have shown that PSK has anticancer potential in adjuvant cancer therapy, with positive results in the treatment of gastric, esophageal, colorectal, breast, and lung cancers.[23–26] These studies suggest that the efficacy of PSK is due to its ability to act as an immunomodulator of biological responses, but the mechanism of action of PSK has not been fully elucidated.

We recently screened for TGF-β inhibitors among commercially available drugs and identified PSK as a strong inhibitor of 3TP-lux, a TGF-β-responsive luciferase reporter. The present study investigated the inhibitory effect of PSK on the TGF-β pathway and TGF-β-induced EMT as possible mechanisms that mediate the anticancer activity of PSK.

Materials and Methods

Cell culture. The human breast epithelial cell line MCF10A was a kind gift from Dr. S. Maheswaran from the Massachusetts General Hospital Cancer Center (Charlestown, MA, USA). The human colorectal cancer cell line SW837, human pancreatic cancer cell line PANC-1, human stomach cancer cell line MKN45, human embryonic kidney cell line HEK293, and monkey kidney cell line COS-1 were obtained from ATCC (Rockville, MD, USA). The culture conditions used for the maintenance of these cell lines have been described previously.[27] Briefly, human pancreatic adenocarcinoma PANC-1, human kidney HEK293, and monkey kidney COS-1 cells were maintained in DMEM (Invitrogen, Carlsbad, CA, USA). Human mammary epithelial MCF10A cells were maintained in DMEM/F12, human gastric cancer MKN-45 cells were maintained in RPMI-1640, and human colorectal cancer SW837 cells were maintained in Leibovitz's L-15 Medium (Invitrogen). All cell culture media were supplemented with 10% FBS (BioWest,

[3]To whom correspondence should be addressed.
E-mail: tetsu@z7.keio.jp

doi: 10.1111/j.1349-7006.2011.02133.x

Nuaillé, France) and 1% penicillin–streptomycin (Invitrogen). Cells were grown in a 5% CO_2 atmosphere at 37°C.

Reagents. Protein-bound polysaccharide, which was supplied by Kureha (Tokyo, Japan), was dissolved with sterilized physiological saline and diluted to the indicated concentrations in the corresponding culture media. Human recombinant TGF-β1 was purchased from R&D Systems (Minneapolis, MN, USA).

Luciferase reporter assay. HEK293 or COS-1 cells (2×10^5) were seeded onto 24-well plates 24 h before transfection. Cells were transiently transfected with the p3TP-lux reporter plasmid (Addgene, Cambridge, MA, USA) and the phRL-TK vector (Promega, Madison, WI, USA) using FuGENE6 (Roche Diagnostics, Indianapolis, IN, USA). After 24 h, the cells were treated with or without 10 ng/mL TGF-β1 for 1 h then cultured in fresh medium in the presence of 0–500 μg/mL PSK. Cell lysates were prepared 24 h later and luciferase activity was assayed by the Dual-Luciferase Reporter System (Promega) and Lumat LB 9501 (Berthold Technologies, Bad Wildbad, Germany). Results were obtained from duplicate wells for each experimental condition and all experiments were carried out in triplicate. p3TP-lux luciferase activity was normalized to that of the control phRL-TK vector.

In order to assay the effects of the constitutively active TGF-β type I receptor, COS-1 cells were seeded at 10 000 cells/well in a 24-well plate and transfected with the p3TP-lux reporter plasmid, the phRL-TK vector, and the pRK5-mutated-TGF β type I receptor (T202D) (Addgene) using FuGENE6. Alternatively, cells were transfected with the p3TP-lux reporter plasmid, the phRL-TK vector, and pRK5 (Addgene) for the negative control. Culture medium was replaced 24 h after transfection and cells were treated with different concentrations of PSK overnight. Cells were harvested after treatment and luciferase assays were carried out. All assays were carried out in triplicate.

Western blot analysis. SW837, MCF10A, PANC-1, and MKN-45 cells were serum-starved for 24 h before treatment with 10 ng/mL TGF-β for 1 h. The cells were subsequently washed and treated with 50–100 μg/mL PSK. After 4 h, cells were lysed in RIPA buffer (Santa Cruz Biotechnology, Santa Cruz, CA, USA) supplemented with a protease inhibitor cocktail (Nacalai Tesque, Kyoto, Japan) and Halt Phosphatase Inhibitor Cocktail (ThermoFisher Scientific, Fremont, CA, USA).

Total protein extracts were analyzed by SDS-PAGE and Wblot analysis with anti-Smad2 (L16D3), anti-phospho-Smad2 (Ser465/467), anti c-Jun (60A8), anti-vimentin (V9) (Abcam, Cambridge, MA, USA), anti-E-cadherin (SHE78-7) (Takara Bio, Shiga, Japan), and anti-phospho-c-Jun (D47G9) antibodies (Cell Signaling Technology, Danvers, MA, USA). Actin, which was used as an internal control, was detected using an anti-actin antibody (C4) (BD Biosciences, San Jose, CA, USA). Immunoreactive proteins were visualized using the ECL Advanced Western Blotting Detection kit (GE Healthcare, Chalfont St Giles, UK).

Quantitative real-time PCR analysis. SW837, MCF10A, and PANC-1 cells were serum-starved for 24 h and subsequently treated with 10 ng/mL TGF-β for 1 h. The cells were washed and cultured in medium containing 50–100 μg/mL PSK for 24 h. Total RNAs were purified from cultured cells using Isogen (Nippon Gene, Tokyo, Japan). First-strand cDNAs were synthesized using the PrimeScript RT reagent kit (Takara Bio) for RT-PCR. Quantitative real-time PCR analysis was carried out using SYBR Premix Ex Taq and the Thermal Cycler Dice Real Time System (Takara Bio).

The following primer sequences were used: human serpin peptidase inhibitor, clade E, member 1 (*SERPINE1*), forward, 5′-CATTACTACGACATCCTGGAACTG-3′, reverse, 5′-AATGTTGGTGAGGGCAGAGAG-3′; human collagen, type1, alpha1 (*COL1A1*), forward, 5′-GTGCTAAAGGTGCCAATGGT-3′, reverse, 5′-ACCAGGTTCACCGCTGTTAC-3′; human transgelin (*TAGLN*), forward, 5′-TCCAGGTCTGGCTGAAGAAT-3′, reverse, 5′-TGCCTTCAAAGAGGTCAACA-3′; human fibronectin 1 (*FN1*), forward, 5′-ACGAGGAAATCTGCACAACC-3′ reverse, 5′-ACACACGTGCACCTCATCAT-3′; and human GAPDH, forward, 5′-GCACCGTCAAGGCTGAGAAC-3′, reverse, 5′-TGGTGAAGACGCCAGTGGA-3′. Human GAPDH was used for normalization. All experiments were carried out in duplicate.

Microscopy. MCF10A cells were cultured in the absence or presence of 2.5 ng/mL TGF-β1 and 500 μg/mL PSK for 11 days. Morphological changes were assessed by an inverted microscope (CKX41; Olympus, Tokyo, Japan) and the images were recorded at ×40 magnification.

Immunohistochemistry. MCF10A cells were cultured in the absence or presence of 2.5 ng/mL TGF-β1 and 50–500 μg/mL PSK for 7 days. Formalin-fixed cells were quenched with Dako REAL peroxidase-blocking solution (Dako, Glostrup, Denmark). Cells were then blocked with Dako Cytomation Protein Block Serum-Free (Dako) and stained with anti-vimentin (V9) (Abcam) or anti-E-cadherin (SHE78-7) (Takara Bio) antibodies, followed by incubation with HRP anti-mouse and anti-rabbit labeled polymers (Dako). Reaction sites were visualized with the EnVision+ kit/HRP (DAB) (Dako) and counterstained with hematoxylin. Images of stained cells were obtained using a digital microscope (VHX-600; Keyence, Osaka, Japan).

Wound healing assay. MCF10A cells were cultured in serum-free medium prior to wounding. Cells that had reached 80% confluency were scratched with a pipette tip, followed by treatment with 10 ng/mL TGF-β and 0–50 μg/mL PSK for 7 h. Phase contrast images were obtained using an inverted microscope (CKX41; Olympus) at a magnification of ×450.

Flow cytometry analysis. MCF10A cells were cultured in the presence or absence of 2.5 ng/mL TGF-β1 and 500 μg/mL PSK for 21 days. Cells were dissociated using PBS-based enzyme-free dissociation buffer (Invitrogen) and centrifuged. Cells were resuspended and stained with anti-CD44-allophycocyanin (APC) mouse monoclonal and anti-CD24-phycoerythrin (PE) (BD Biosciences) antibodies on ice for 30 min. Samples were then resuspended in PBS containing 2% FBS and examined using a FACSCalibur flow cytometer (BD Biosciences). APC-IgG and PE-IgG antibodies were used as controls. No-antibody and single-antibody controls were used to normalize the sample readings and to designate quadrants. The results were analyzed using CellQuest software (BD Biosciences).

Mammosphere culture. MCF10A cells were cultured in DMEM/F12 media with or without 10 ng/mL TGF-β1 or 500 μg/mL PSK for 12 days. Single-cell suspension cultures were prepared at a densities of 40 000, 20 000, 10 000, 5000, 2500, and 1250 cells per well in DMEM/F-12 supplemented with 2% B27 (Invitrogen), 20 ng/mL epidermal growth factor, and 20 ng/mL basic fibroblast growth factor (BD Biosciences) and seeded into six-well ultra low attachment plates (2.5 mL per plate). Culture medium was fed on day 4 and day 6, and the number of mammospheres was recorded 9 days after the start of the culture period.[28,29]

Statistical analysis. Statistical differences were determined for *in vitro* assays by Student's *t*-test. Data were analyzed using SPSS software (SPSS, Chicago, IL, USA). We considered values of $P < 0.05$ statistically significant and values of $P < 0.01$ highly significant.

Results

Inhibition of the TGF-β-responsive luciferase reporter by PSK treatment. Protein-bound polysaccharide-induced inhibition of the TGF-β pathway was investigated in HEK293 and COS-1 cells using the 3TP-lux luciferase reporter assay. 3TP-lux is a TGF-β1-responsive luciferase reporter gene that contains three

doi: 10.1111/j.1349-7006.2011.02133.x

consecutive tetradecanoylphorbol acetate response elements and a portion of the plasminogen activator inhibitor 1 (PAI-1/SERPINE1) promoter region.[30] The signal intensity was normalized by *Renilla* luciferase. After 24 h of serum starvation, the luciferase activities of 3TP-lux were increased in both cell lines after treatment with TGF-β1; however, 3TP-lux activity was suppressed in response to PSK treatment in a dose-dependent manner (Fig. 1A). Moreover, we examined the 3TP-lux activity of COS-1 cells that expressed the constitutively active mutant of TGF-β type I receptor (active TGF-βRI). As expected, 3TP-lux activity was increased by transfection of active TGF-βRI as well as by TGF-β1 treatment; however, 3TP-lux activity was suppressed after PSK treatment (Fig. 1B). It was previously reported that PSK selectively binds and reduces the active form of TGF-β1.[31] However, our results suggest that PSK inhibits signaling downstream of TGF-β receptors in addition to neutralizing TGF-β1.

Protein-bound polysaccharide inhibits Smad signaling and expression of TGF-β-signaling target genes. To determine whether PSK suppresses the Smad pathway,[32] SW837, MCF10A, PANC-1, and MKN45 cell lines with normal Smad2 expression and non-mutated TGF-β receptors[33,34] were treated with TGF-β1 after 24 h of serum starvation. Cells were subsequently treated with several concentrations of PSK for 4 h after TGF-β1 depletion and Smad2 phosphorylation was examined by immunoblotting. Western blot analysis showed a trend of PSK suppression of TGF-β1-induced Smad2 phosphorylation in a dose-dependent manner (Fig. 1C).

Transforming growth factor-β signaling activates target genes such as *FN1*, *SERPINE1*, *TAGLN*, and *COL1A1*. *FN1* plays an important role in development and wound healing by promoting cell adhesion, migration, and cytoskeletal organization.[35] *SERPINE1* regulates tumor cell invasion through the precise regulation of the peritumoral proteolytic microenvironment. *TAGLN* expression is required for epithelial cell proliferation and migration and is implicated in the regulation of fibrosis.[36] *COL1A1* is the major fibrous collagen synthesized by wound fibroblasts during the repair process.[37] In the present study, the mRNA levels of *FN1*, *SERPINE1*, *TAGLN*, and *COL1A1* were determined by quantitative RT-PCR. The mRNA levels of these downstream target genes of TGF-β1 signaling were elevated by TGF-β1 treatment after 24 h serum starvation in SW837, MCF10A, and PANC-1 cells. Treatment with PSK showed a dose-dependent tendency to decrease the mRNA levels of these target genes (Fig. 2, Fig. S1).

In addition to its effect on Smad signaling, TGF-β1 also activates the MAPK pathway, including ERK, JNK, and p38 kinase.[38,39] SW837 cells were serum-starved for 24 h, treated with TGF-β1, and treated with several concentrations of PSK for 4 h after TGF-β1 depletion. c-Jun phosphorylation was

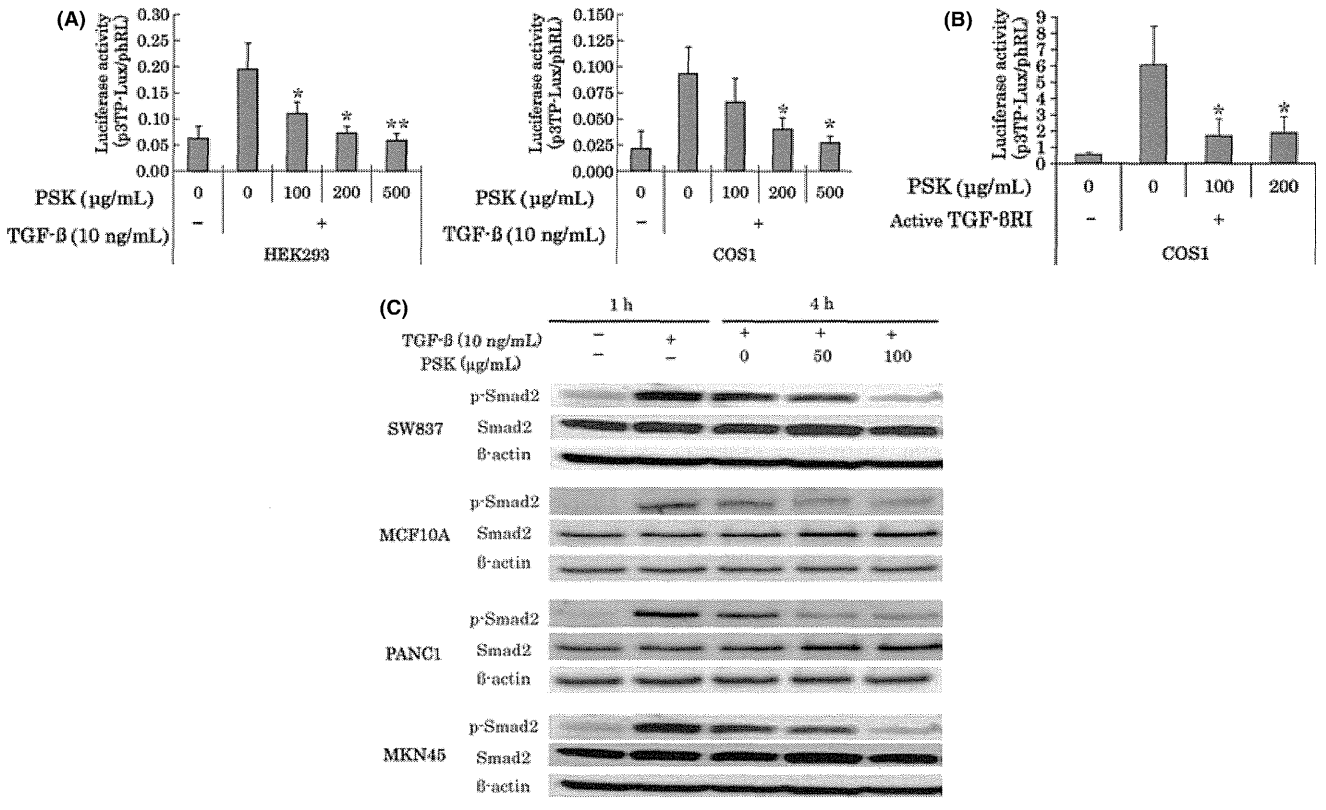

Fig. 1. (A,B) Protein-bound polysaccharide (PSK) inhibits transforming growth factor-β (TGF-β) activity. (A) HEK293 and COS-1 cells were seeded in 24-well plates and transiently transfected with the p3TP-lux reporter plasmid. (B) COS-1 cells were seeded in 24-well plates and transfected with the p3TP-lux reporter plasmid, the phRL-TK vector, and the pRK5-mutated-TGF-β type I receptor (T202D). After 24 h, cells were treated with or without TGF-β1 for 1 h before treatment with various concentrations of PSK for 24 h. Cells were then harvested for analysis of luciferase activity. The results were obtained from duplicate wells and the data points are the averages of three independent experiments. The error bars represent SD. Differences in the $TGF\text{-}\beta^{+}$ and PSK^{-} groups were compared by Student's *t*-test; statistically significant at $^{*}P < 0.05$ or $^{**}P < 0.01$. (C) PSK suppresses TGF-β-activated p-Smad2. Colon (SW837), breast (MCF10A), pancreatic (PANC-1), and gastric cancer (MKN45) cell lines expressing normal levels of Smad2 and wild-type TGF-β receptor were treated with TGF-β1 for 1 h after 24 h of serum starvation. Smad2 phosphorylation was examined by immunoblotting after 4 h of treatment with several concentrations of PSK.

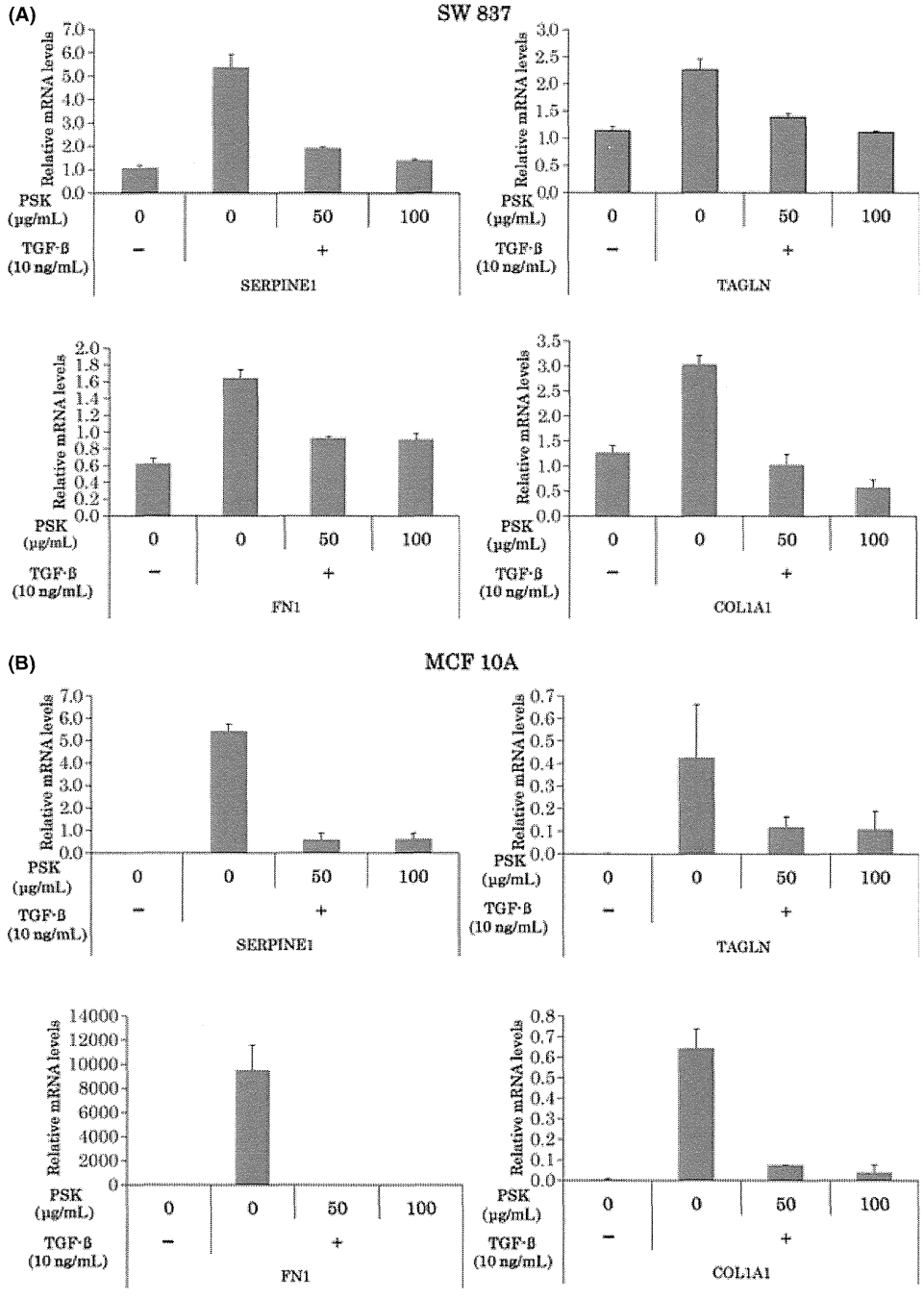

Fig. 2. Protein-bound polysaccharide (PSK) represses the expression of transforming growth factor-β (TGF-β) target mRNAs. The transcript levels of TGF-β target genes were measured in SW837 and MCF10A cells using quantitative real-time PCR. Cells were treated with or without TGF-β1 and various concentrations of PSK. The mRNA levels of *FN1*, *SERPINE1*, *TAGLIN*, and *COL1A1* were repressed by PSK treatment in a dose-dependent manner. The data are reported as the mean ± SD.

subsequently examined by immunoblotting. Unexpectedly, TGF-β1 treatment increased the levels of both c-Jun and phosphorylated c-Jun; however, PSK treatment decreased both c-Jun and phosphorylated c-Jun levels in a dose-dependent manner (Fig. S2).

Protein-bound polysaccharide inhibits EMT induced by activation of TGF-β pathway. The EMT process, which is a crucial step in tumor progression, can be induced by several cytokines and chemokines, including TGF-β.[40] After 7 days of treatment with TGF-β1, immortalized human mammary epithelial MCF10A cells showed a change in phenotype, becoming spindle-shaped with loose cell–cell contacts. However, MCF10A cells co-cultured with TGF-β1 and PSK did not show phenotypic changes and maintained epithelial characteristics (Fig. 3A).

Immunohistochemical analysis showed that E-cadherin expression was inhibited in TGF-β1-treated MCF10A cells after 7 days, but no changes in expression were detected when the cells were co-cultured with PSK. Moreover, the TGF-

doi: 10.1111/j.1349-7006.2011.02133.x

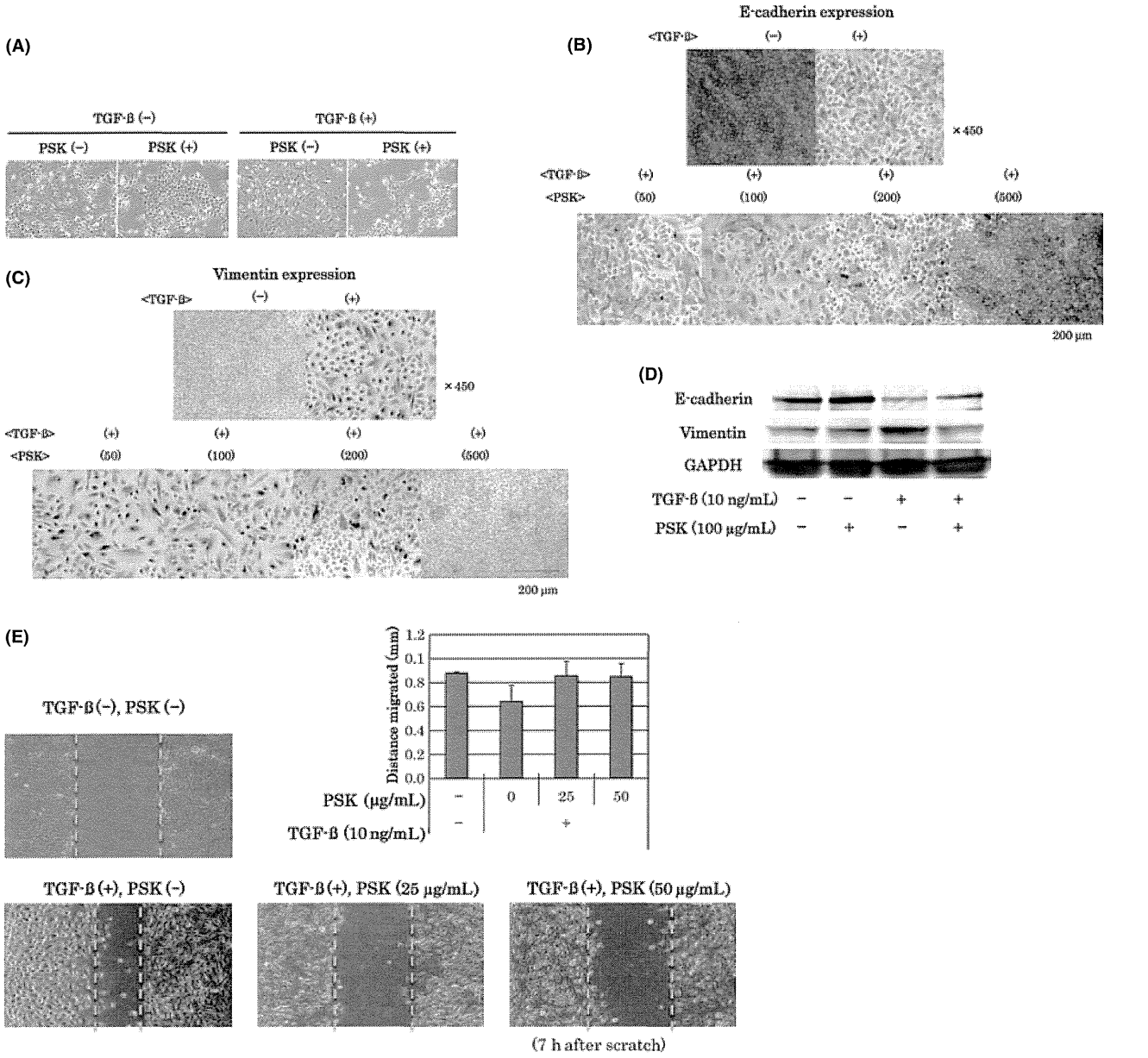

Fig. 3. (A) Protein-bound polysaccharide (PSK) inhibits transforming growth factor-β (TGF-β)-mediated epithelial–mesenchymal transition. Treatment with TGF-β1 for 7 days in MCF10A cells resulted in phenotypic changes. The TGF-β1-treated MCF10A cells were spindle-shaped with loose cell–cell contacts, whereas MCF10A cells co-cultured with TGF-β1 and PSK did not show phenotypic changes and showed a typical cobblestone appearance. (B,C) Immunohistochemical detection of vimentin and E-cadherin in MCF10A cells in the absence or presence of TGF-β1 and various concentrations of PSK for 7 days in serum-free medium. (D) Vimentin and E-cadherin expression were examined by immunoblotting after 4 h of treatment with TGF-β and/or PSK in MCF10A cells. (E) Migratory behavior of MCF10A cells in the absence or presence of TGF-β and PSK. MCF10A cells were stimulated with or without TGF-β or various concentrations of PSK and migratory behavior was analyzed in an *in vitro* wound model. Cells grown to 80% confluency were scratched by a pipette tip and photographs were taken immediately after the incision and after 7 h.

β1-induced upregulation of vimentin expression was diminished by PSK (Fig. 3B,C). Western blot analysis showed that PSK treatment inhibited both the TGF-β1 treatment-induced downregulation of E-cadherin expression and the upregulation of vimentin expression, suggesting that PSK suppresses TGF-β1-induced EMT (Fig. 3D).

The migratory ability of MCF10A cells stimulated with or without TGF-β or various concentrations of PSK was analyzed using a wound healing assay. Cultured cells reaching 80% confluency were pretreated with mitomycin C and scratched with a pipette tip, and the length of the wound was measured immediately after the incision and after 7 h of incubation with 10 ng/mL TGF-β and 0–50 μg/mL PSK (Fig. 3E). MCF10A cells did not show any migratory ability in the absence of EMT.[27] These results showed that MCF10A cells acquired a higher migratory ability in response to TGF-β1 treatment and this ability was abolished when these cells were treated with PSK.

Mani *et al.*[29] reported that the induction of EMT factors such as TGF-β1 in human mammary epithelial cells was associated with the acquisition of mesenchymal morphology and the expression of mesenchymal markers. This phenotypic EMT change increased the $CD44^+/CD24^-$ cell subpopulation, which showed the properties of their mammary epithelial progenitors and an enhanced mammosphere-forming ability. In the present study, FACS analysis of the cell-surface markers CD44 and CD24 in the mammary epithelial cell line MCF10A showed that TGF-β1 treatment increased the $CD44^+/CD24^-$ cell population from 1.98% to 18.6%. However, the $CD44^+/CD24^-$ cell population did not change in MCF10A cells co-cultured with PSK (Fig. 4A), indicating that PSK inhibits the EMT-mediated generation of the $CD44^+/CD24^-$ population. The mammosphere formation assay in MCF10A cells showed that TGF-β1 treatment triggered the formation of mammospheres, whereas mammosphere formation was decreased in cells that were not treated with TGF-β1 or co-treated with TGF-β1 and PSK (Fig. 4B).

Discussion

Protein-bound polysaccharide has been used as a non-specific immunostimulant for the treatment of cancer patients in Japan for more than 30 years without the occurrence of adverse side-effects. The antitumor activity of PSK has been documented in various experimental models and beneficial therapeutic effects were shown in several types of tumors in clinical studies. The addition of PSK to adjuvant chemotherapy significantly prolonged survival after curative surgery in a large prospective trial of patients with gastric and colorectal cancer.[23,25] Protein-bound polysaccharide is a non-specific immunopotentiator that exerts immunomodulatory action by inducing the production of interleukin-2 and γ-interferon, thereby stimulating lymphokine-activated killer cells and enhancing natural killer cells.[41] Proetin-bound polysaccharide also has a favorable effect on the activation of leukocyte chemotactic locomotion and phagocytic activity.[42,43] Moreover, it was recently revealed that PSK is a specific Toll-like receptor 2 agonist and has potent antitumor

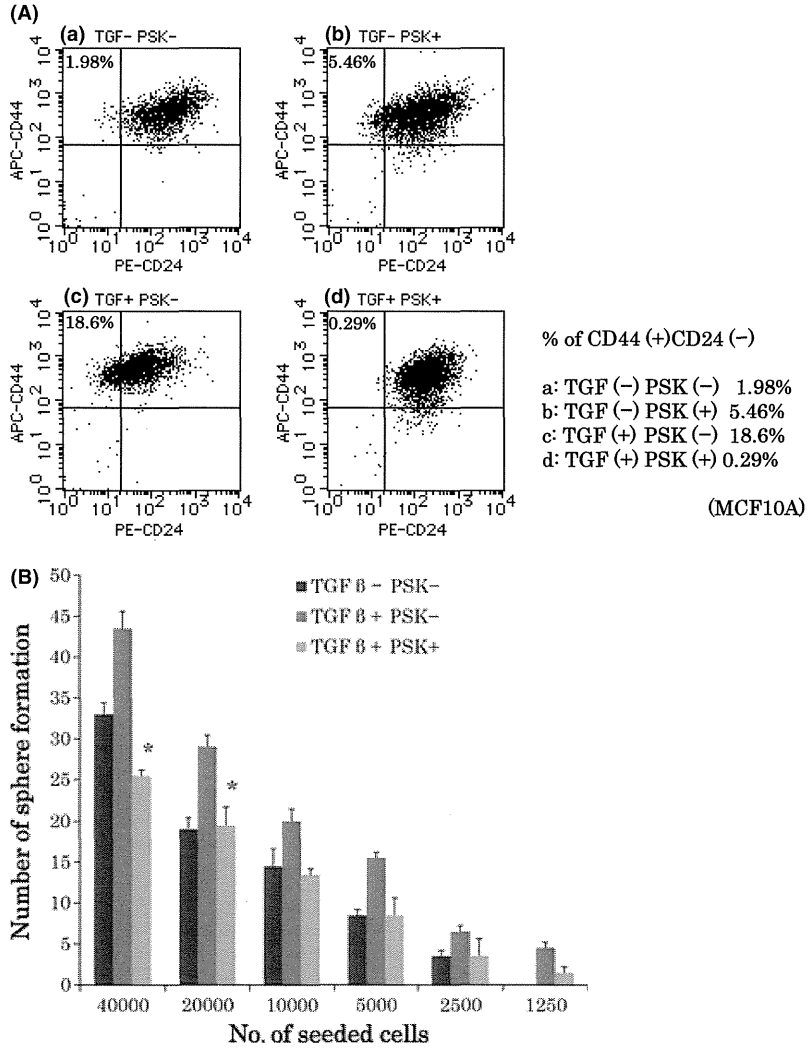

Fig. 4. (A) Fluorescence-activated cell sorting analysis of the cell-surface markers CD44 and CD24 in the MCF10A mammary epithelial cell line. (B) *In vitro* quantification of mammospheres formed by MCF10A cells. The data are reported as the number of mammospheres formed/various numbers of seeded cells after 9 days of treatment with transforming growth factor-β (TGF-β) and/or protein-bound polysaccharide (PSK). The data are reported as the mean ± SD. Differences in the TGF-β(+) and PSK(–) groups were compared by Student's *t*-test. There were statistically significant differences at a *P*-value of <0.05.

doi: 10.1111/j.1349-7006.2011.02133.x

effects through stimulation of both $CD8^+$ T cells and natural killer cells.[44]

The anticancer effect of PSK might involve a direct regulatory action on growth factor production and enzyme activity in tumors in addition to the immunomodulatory activities mentioned above. Zhang *et al.*[31] reported that PSK selectively bound and reduced the active form of TGF-β1, thereby inhibiting tumor invasiveness through direct inhibition of TGF-β1 production, MMPs, and the urokinase-type plasminogen activator system. In this study, we showed the inhibitory effect of PSK on the TGF-β pathway and TGF-β-induced EMT.

In the present study, PSK inhibited the Smad pathway, the major regulator of TGF-β signaling,[38] by suppressing Smad2 protein phosphorylation. Protein-bound polysaccharide also decreased the levels of both c-Jun and phosphorylated c-Jun, which were increased by TGF-β1 treatment, suggesting that the effect of PSK involves the MAPK pathway. Treatment with PSK inhibited the expression of several TGF-β pathway target genes and prevented TGF-β1-induced EMT. These findings indicate that PSK inhibits TGF-β-associated pathways such as Smad and MAPK signaling even if these pathways have been activated, and the ability of PSK to inhibit these pathways suggests that it acts upstream of Smad and MAPK signaling. Although the interaction between PSK and TGF-β receptors was evaluated by immunoprecipitation, the results were inconclusive because the PSK extracted from the fungus *C. versicolor* exists as a glycoprotein complex rather than a single molecule. Thus, an additional study should be undertaken to clarify the biological mechanism of PSK action.

Various TGF-β signaling inhibitors, including antisense oligonucleotides against TGF-β2,[45–47] mAb against TGF-β,[48–50] and small molecule inhibitors,[51] have recently been developed. Among them, a soluble antisense oligonucleotide that is specific for human TGF-β2 mRNA, AP12009, has been used to target the TGF-β pathway *in vivo* and is currently in clinical trials for malignant gliomas.[45,46] A phase II study of Belagenpumatucel-L, a TGF-β2 antisense gene-modified allogeneic tumor cell vaccine for non-small-cell lung cancer, suggested that this compound provided a survival advantage and was well tolerated; therefore, this agent should be investigated further. In addition, mAbs to TGF-β are currently in clinical trials including CAT-152, which is used to prevent the progression of fibrosis after trabeculectomy for primary open-angle or chronic angle-closure glaucoma,[48] and CAT-192, which is used to treat early-stage diffuse cutaneous systemic sclerosis.[49]

Although the results obtained with TGF-β inhibitors in clinical trials are promising, TGF-β-based therapeutic strategies must be carefully considered in each case. Because a large number of cellular context-dependent factors contribute to the dynamic regulatory roles of TGF-β signaling, an alteration of this balance could have a significant effect on the characteristics of certain cells and induce oncogenic transformation. The potentially deleterious effects of these strategies in normal tissues must be considered.

In the 30-year history of its clinical use, PSK has not shown severe side-effects, and it has prolonged the survival of cancer patients and reduced the recurrence of tumors.[23,25] The anticancer activities of PSK are reportedly derived from its immunomodulatory effects and its inhibitory effect on TGF-β. The present data, which confirm the inhibition of the TGF-β pathway by PSK, suggest that this agent is not only effective as an anticancer drug but could also be applied as a TGF-β inhibitor in diseases caused by the aberrant activation of the TGF-β pathway such as primary open-angle glaucoma, diffuse cutaneous systemic sclerosis, and pulmonary fibrosis.

In conclusion, the present results show the effect of PSK on TGF-β pathway inhibition and indicate that PSK could be a promising new agent for the treatment of diseases associated with alterations in TGF-β signaling.

Acknowledgments

This research was supported by the Japanese Ministry of Education, Culture, Sports, Science and Technology Grant-in-Aid for Scientific Research (B) (#21791260 T.H.) and a Grant-in-Aid for the Global Center of Excellence (COE) Program entitled "Education and Research Center for Stem Cell Medicine" (Keio University, Tokyo, Japan).

Disclosure Statement

The authors have no conflicts of interest.

References

1 Miyazono K, Suzuki H, Imamura T. Regulation of TGF-beta signaling and its roles in progression of tumors. *Cancer Sci* 2003; **94**: 230–4.
2 Siegel PM, Massague J. Cytostatic and apoptotic actions of TGF-beta in homeostasis and cancer. *Nat Rev Cancer* 2003; **3**: 807–21.
3 Bierie B, Moses HL. TGF-beta and cancer. *Cytokine Growth Factor Rev* 2006; **17**: 29–40.
4 Massague J. TGFbeta in Cancer. *Cell* 2008; **134**: 215–30.
5 Xu J, Lamouille S, Derynck R. TGF-beta-induced epithelial to mesenchymal transition. *Cell Res* 2009; **19**: 156–72.
6 Derynck R, Akhurst RJ, Balmain A. TGF-beta signaling in tumor suppression and cancer progression. *Nat Genet* 2001; **29**: 117–29.
7 Dumont N, Arteaga CL. Targeting the TGF beta signaling network in human neoplasia. *Cancer Cell* 2003; **3**: 531–6.
8 Ikushima H, Miyazono K. TGFbeta signalling: a complex web in cancer progression. *Nat Rev Cancer* 2010; **10**: 415–24.
9 Ivanovic V, Melman A, Davis-Joseph B, Valcic M, Geliebter J. Elevated plasma levels of TGF-beta 1 in patients with invasive prostate cancer. *Nat Med* 1995; **1**: 282–4.
10 Bandyopadhyay A, Agyin JK, Wang L *et al.* Inhibition of pulmonary and skeletal metastasis by a transforming growth factor-beta type I receptor kinase inhibitor. *Cancer Res* 2006; **66**: 6714–21.
11 Ehata S, Hanyu A, Fujime M *et al.* Ki26894, a novel transforming growth factor-beta type I receptor kinase inhibitor, inhibits in vitro invasion and in vivo bone metastasis of a human breast cancer cell line. *Cancer Sci* 2007; **98**: 127–33.
12 Naka K, Hoshii T, Muraguchi T *et al.* TGF-beta-FOXO signalling maintains leukaemia-initiating cells in chronic myeloid leukaemia. *Nature* 2010; **463**: 676–80.
13 Ikushima H, Todo T, Ino Y, Takahashi M, Miyazawa K, Miyazono K. Autocrine TGF-beta signaling maintains tumorigenicity of glioma-initiating cells through Sry-related HMG-box factors. *Cell Stem Cell* 2009; **5**: 504–14.
14 Maehara Y, Kakeji Y, Kabashima A *et al.* Role of transforming growth factor-beta 1 in invasion and metastasis in gastric carcinoma. *J Clin Oncol* 1999; **17**: 607–14.
15 Saito H, Tsujitani S, Oka S *et al.* An elevated serum level of transforming growth factor-beta 1 (TGF-beta 1) significantly correlated with lymph node metastasis and poor prognosis in patients with gastric carcinoma. *Anticancer Res* 2000; **20**: 4489–93.
16 Ghellal A, Li C, Hayes M, Byrne G, Bundred N, Kumar S. Prognostic significance of TGF beta 1 and TGF beta 3 in human breast carcinoma. *Anticancer Res* 2000; **20**: 4413–18.
17 Elliott RL, Blobe GC. Role of transforming growth factor Beta in human cancer. *J Clin Oncol* 2005; **23**: 2078–93.
18 Zhang B, Halder SK, Zhang S, Datta PK. Targeting transforming growth factor-beta signaling in liver metastasis of colon cancer. *Cancer Lett* 2009; **277**: 114–20.
19 Matsunaga K, Hosokawa A, Oohara M, Sugita N, Harada M, Nomoto K. Direct action of a protein-bound polysaccharide, PSK, on transforming growth factor-beta. *Immunopharmacology* 1998; **40**: 219–30.
20 Nakazato H, Koike A, Saji S, Ogawa N, Sakamoto J. Efficacy of immunochemotherapy as adjuvant treatment after curative resection of gastric

cancer. Study Group of Immunochemotherapy with PSK for Gastric Cancer. *Lancet* 1994; **343**: 1122–6.
21 Ohwada S, Ikeya T, Yokomori T *et al.* Adjuvant immunochemotherapy with oral Tegafur/Uracil plus PSK in patients with stage II or III colorectal cancer: a randomised controlled study. *Br J Cancer* 2004; **90**: 1003–10.
22 Katoh R, Ooshiro M. Enhancement of antitumor effect of tegafur/uracil (UFT) plus leucovorin by combined treatment with protein-bound polysaccharide, PSK, in mouse models. *Cell Mol Immunol* 2007; **4**: 295–9.
23 Sakamoto J, Morita S, Oba K *et al.* Efficacy of adjuvant immunochemotherapy with polysaccharide K for patients with curatively resected colorectal cancer: a meta-analysis of centrally randomized controlled clinical trials. *Cancer Immunol Immunother* 2006; **55**: 404–11.
24 Ogoshi K, Satou H, Isono K, Mitomi T, Endoh M, Sugita M. Immunotherapy for esophageal cancer. A randomized trial in combination with radiotherapy and radiochemotherapy. Cooperative Study Group for Esophageal Cancer in Japan. *Am J Clin Oncol* 1995; **18**: 216–22.
25 Ueda Y, Fujimura T, Kinami S *et al.* A randomized phase III trial of postoperative adjuvant therapy with S-1 alone versus S-1 plus PSK for stage II/IIIA gastric cancer: Hokuriku-Kinki Immunochemo-Therapy Study Group-Gastric Cancer (HKIT-GC). *Jpn J Clin Oncol* 2006; **36**: 519–22.
26 Kidd PM. The use of mushroom glucans and proteoglycans in cancer treatment. *Altern Med Rev* 2000; **5**: 4–27.
27 Hayashida T, Takahashi F, Chiba N *et al.* HOXB9, a gene overexpressed in breast cancer, promotes tumorigenicity and lung metastasis. *Proc Natl Acad Sci U S A* 2010; **107**: 1100–5.
28 Grimshaw MJ, Cooper L, Papazisis K *et al.* Mammosphere culture of metastatic breast cancer cells enriches for tumorigenic breast cancer cells. *Breast Cancer Res* 2008; **10**: R52.
29 Mani SA, Guo W, Liao MJ *et al.* The epithelial–mesenchymal transition generates cells with properties of stem cells. *Cell* 2008; **133**: 704–15.
30 Wrana JL, Attisano L, Carcamo J *et al.* TGF beta signals through a heteromeric protein kinase receptor complex. *Cell* 1992; **71**: 1003–14.
31 Zhang H, Morisaki T, Matsunaga H *et al.* Protein-bound polysaccharide PSK inhibits tumor invasiveness by down-regulation of TGF-beta1 and MMPs. *Clin Exp Metastasis* 2000; **18**: 343–52.
32 Massague J, Chen YG. Controlling TGF-beta signaling. *Genes Dev* 2000; **14**: 627–44.
33 Geismann C, Morscheck M, Koch D *et al.* Up-regulation of L1CAM in pancreatic duct cells is transforming growth factor beta1- and slug-dependent: role in malignant transformation of pancreatic cancer. *Cancer Res* 2009; **69**: 4517–26.
34 Ganapathy V, Ge R, Grazioli A *et al.* Targeting the transforming growth factor-beta pathway inhibits human basal-like breast cancer metastasis. *Mol Cancer* 2010; **9**: 122.
35 Hocevar BA, Brown TL, Howe PH. TGF-beta induces fibronectin synthesis through a c-Jun N-terminal kinase-dependent, Smad4-independent pathway. *EMBO J* 1999; **18**: 1345–56.
36 Cutroneo KR, White SL, Phan SH, Ehrlich HP. Therapies for bleomycin induced lung fibrosis through regulation of TGF-beta1 induced collagen gene expression. *J Cell Physiol* 2007; **211**: 585–9.
37 Yu H, Konigshoff M, Jayachandran A *et al.* Transgelin is a direct target of TGF-beta/Smad3-dependent epithelial cell migration in lung fibrosis. *FASEB J* 2008; **22**: 1778–89.
38 Shi Y, Massague J. Mechanisms of TGF-beta signaling from cell membrane to the nucleus. *Cell* 2003; **113**: 685–700.
39 Lim IJ, Phan TT, Tan EK *et al.* Synchronous activation of ERK and phosphatidylinositol 3-kinase pathways is required for collagen and extracellular matrix production in keloids. *J Biol Chem* 2003; **278**: 40851–8.
40 Nawshad A, LaGamba D, Hay ED. Transforming growth factor beta (TGFbeta) signalling in palatal growth, apoptosis and epithelial mesenchymal transformation (EMT). *Arch Oral Biol* 2004; **49**: 675–89.
41 Harada M, Matsunaga K, Oguchi Y *et al.* Oral administration of PSK can improve the impaired anti-tumor CD4+ T-cell response in gut-associated lymphoid tissue (GALT) of specific-pathogen-free mice. *Int J Cancer* 1997; **70**: 362–72.
42 Torisu M, Hayashi Y, Ishimitsu T *et al.* Significant prolongation of disease-free period gained by oral polysaccharide K (PSK) administration after curative surgical operation of colorectal cancer. *Cancer Immunol Immunother* 1990; **31**: 261–8.
43 Price LA, Wenner CA, Sloper DT, Slaton JW, Novack JP. Role for toll-like receptor 4 in TNF-alpha secretion by murine macrophages in response to polysaccharide Krestin, a *Trametes versicolor* mushroom extract. *Fitoterapia* 2010; **81**: 914–19.
44 Lu H, Yang Y, Gad E *et al.* Polysaccharide krestin is a novel TLR2 agonist that mediates inhibition of tumor growth via stimulation of CD8 T cells and NK cells. *Clin Cancer Res* 2011; **17**: 67–76.
45 Schlingensiepen KH, Schlingensiepen R, Steinbrecher A *et al.* Targeted tumor therapy with the TGF-beta 2 antisense compound AP 12009. *Cytokine Growth Factor Rev* 2006; **17**: 129–39.
46 Hau P, Jachimczak P, Schlingensiepen R *et al.* Inhibition of TGF-beta2 with AP 12009 in recurrent malignant gliomas: from preclinical to phase I/II studies. *Oligonucleotides* 2007; **17**: 201–12.
47 Nemunaitis J, Dillman RO, Schwarzenberger PO *et al.* Phase II study of belagenpumatucel-L, a transforming growth factor beta-2 antisense gene-modified allogeneic tumor cell vaccine in non-small-cell lung cancer. *J Clin Oncol* 2006; **24**: 4721–30.
48 Khaw P, Grehn F, Hollo G *et al.* A phase III study of subconjunctival human anti-transforming growth factor beta(2) monoclonal antibody (CAT-152) to prevent scarring after first-time trabeculectomy. *Ophthalmology* 2007; **114**: 1822–30.
49 Denton CP, Merkel PA, Furst DE *et al.* Recombinant human anti-transforming growth factor beta1 antibody therapy in systemic sclerosis: a multicenter, randomized, placebo-controlled phase I/II trial of CAT-192. *Arthritis Rheum* 2007; **56**: 323–33.
50 Wormstone IM, Anderson IK, Eldred JA, Dawes LJ, Duncan G. Short-term exposure to transforming growth factor beta induces long-term fibrotic responses. *Exp Eye Res* 2006; **83**: 1238–45.
51 Tojo M, Hamashima Y, Hanyu A *et al.* The ALK-5 inhibitor A-83-01 inhibits Smad signaling and epithelial-to-mesenchymal transition by transforming growth factor-beta. *Cancer Sci* 2005; **96**: 791–800.

Supporting Information

Additional Supporting Information may be found in the online version of this article:

Fig. S1. Protein-bound polysaccharide (PSK) inhibits the expression of transforming growth factor-β (TGF-β) signaling target genes.

Fig. S2. Protein-bound polysaccharide (PSK) suppresses transforming growth factor-β (TGF-β)-activated p-c-Jun.

Please note: Wiley-Blackwell are not responsible for the content or functionality of any supporting materials supplied by the authors. Any queries (other than missing material) should be directed to the corresponding author for the article.

doi: 10.1111/j.1349-7006.2011.02133.x

Original Article

Eur Surg (2012) 44/4: 267–273
DOI 10.1007/s10353-012-0082-y

european surgery
ACA Acta Chirurgica Austriaca
Printed in Austria

Risk factor analysis and procedural modifications for biliary stricture after adult living donor liver transplantation

M. Shinoda[1], M. Tanabe[1], S. Kawachi[1], O. Itano[1], H. Obara[1], T. Hibi[1], K. Matsubara[1], N. Shimojima[2], Y. Fuchimoto[2], K. Hoshino[2], G. Wakabayashi[3], M. Shimazu[4], Y. Morikawa[2], M. Kitajima[5], Y. Kitagawa[1]

[1]Department of Surgery, Keio University School of Medicine, Tokyo, Japan
[2]Department of Pediatric Surgery, Keio University School of Medicine, Tokyo, Japan
[3]Department of Surgery, Iwate Medical University School of Medicine, Iwate, Japan
[4]Department of Digestive Surgery, Hachioji Medical Center of Tokyo Medical University, Tokyo, Japan
[5]International University Health and Welfare Mita Hospital, Tokyo, Japan

Received April 25, 2011; accepted after revision January 20, 2012; published online May 3, 2012

Summary. *Background:* We undertook a retrospective assessment of risk factors for biliary stricture after adult living donor liver transplantation (LDLT) and evaluated risk reduction following the implementation of modified surgical procedures.

Methods: Between June 1997 and December 2009, 85 adult patients underwent LDLT. Up to September 2006, we performed duct-to-duct hepaticocholedochostomy (D-D) in 38 patients and Roux-en-Y hepaticojejunostomy (R-Y) in 24 patients. Risk factors for biliary stricture were analyzed for these patients. We then performed D-D in 23 patients using modified procedures and assessed the resultant outcomes.

Results: D-D was a significant risk factor in the 62 patients who underwent LDLT before September 2006. Despite this result, we decided to employ only D-D for subsequent cases. Since the presence of multiple graft bile duct orifices was a significant risk factor in the 38 patients who underwent D-D, we used modified procedures after October 2006 to address grafts with multiple bile duct orifices. The procedures included: 1) inserting a biliary tube from the common bile duct; 2) placing the tip of tube beyond the anastomosis; 3) inserting the tubes in all the anastomoses if multiple; and 4) maintaining the tube for 6 months postoperatively. The incidence of biliary stricture after D-D was significantly less frequent with the use of these procedures (before: 36%; after: 13%).

Conclusions: In our early experience, D-D was a significant risk factor for biliary stricture after adult LDLT. Although we are now employing only D-D, our procedural modifications seem promising for preventing biliary stricture after D-D.

Keywords: Biliary stricture, living donor liver transplantation, risk factor, biliary tube.

Abbreviations

LDLT	living donor liver transplantation
D-D	duct-to-duct hepaticocholedochostomy
R-Y	Roux-en-Y hepaticojejunostomy
GW/RBW	graft-to-recipient weight ratio
PDS	polydioxanone suture

Introduction

Biliary stricture is one of the most serious complications that can arise after living donor liver transplantation (LDLT). In our initial LDLT cases, we employed both duct-to-duct hepaticocholedochostomy (D-D) and Roux-en-Y hepaticojejunostomy (R-Y) for biliary reconstruction, and found that the incidence of biliary stricture in patients that underwent D-D was higher than in those that underwent R-Y in 2002 [1]. For these initial cases, we paid attention to various possible complications and did not focus on biliary stricture in particular. In light of the higher incidence of biliary stricture in patients with D-D, we began to pay greater attention to the prevention of biliary stricture. Our chief considerations at that point included selection of the biliary reconstruction method, procedures for placing the biliary drainage tube, and postoperative management of the tube. Subsequently, we modified our surgical procedure based on these considerations. However, as of 2006, these modifications had

Correspondence: Minoru Tanabe, MD, Ph.D., Department of Surgery, Keio University School of Medicine, 35 Shinanomachi, Shinjuku-ku, Tokyo 160-8582, Japan.
Fax: ++81-3355-4707
E-mail: m-tanabe@ab.keio.jp

not resulted in any noticeable improvements in the incidence of biliary stricture. In 2006, we retrospectively analyzed risk factors for biliary stricture after adult LDLT to obtain evidence that could serve to identify strategies to reduce the incidence of biliary stricture, and we further modified our procedures for biliary tube placement and postoperative management based on the result of these analyses. In this study, we present the results of the risk factor analysis for patients enrolled before 2006 and assess whether the subsequent procedural modifications resulted in an improvement in the incidence of biliary stricture.

Patients and methods

Risk factor analyses

Between June 1997 and December 2009, 85 adult patients underwent LDLT at Keio University Hospital, Japan, and survived more than 1 month after the operation. Up to September 2006, we performed 62 LDLTs, employing D-D in 38 patients and R-Y in 24 patients. The patient characteristics are shown in Table 1. In these 62 patients, the relationship between biliary stricture and the following factors was analyzed: recipient age, donor age, graft-to-recipient weight ratio (GW/RBW), ABO blood type incompatibility, post-operative anastomotic bile leakage, post-operative acute cellular rejection, post-operative intra-abdominal bleeding, recipient gender, method of biliary reconstruction, type of graft, and number of orifices in the graft. We performed the same analyses employing only the 38 patients for whom we performed D-D; the relationship between biliary stricture and the factors above, except biliary reconstruction, was analyzed.

Diagnosis of biliary stricture

A diagnosis of anastomotic biliary stricture was reached if both elevation of serum transaminases and stenosis were

Tab. 1: Characteristics of the 62 patients subjected to risk factor analysis

		–2006.9 Total ($n=62$)	–2006.9 D-D ($n=38$)	–2006.9 R-Y ($n=24$)
Recipient gender	Male	36 (58%)	22 (58%)	14 (58%)
	Female	26 (42%)	16 (42%)	10 (42%)
Mean recipient age (y)		44.4±12.2 (19–64)	46.4±11.5 (21 –64)	41.1±12.9 (19–60)
Mean donor age (y)		41.0±14.1 (19–65)	40.3±12.5 (120–65)	42.0±16.4 (19–64)
Mean follow-up period (m)		44.5±29.8 (3–116)	38.0±26.0 (3–80)	57.7±32.2 (12–116)
Disease	Liver cirrhosis (viral, alcoholic)	26	19	7
	Acute liver failure	12	1	1
	Primary biliary cirrhosis	10	6	4
	Primary sclerosing cholangitis	3	0	3
	Biliary atresia	3	0	3
	Secondary biliary cirrhosis	2	0	2
	Auto-immune hepatitis	1	0	1
	Familial amyloid polyneuropathy	1	0	1
	Nonalcoholic steatohepatitis	1	1	0
	Caroli's syndrome	1	0	1
	Metastatic liver tumor	1	0	1
	Wilson's disease	1	0	1
ABO compatibility	Not-incompatible	51 (82%)	30 (79%)	21 (88%)
	Incompatible	11 (18%)	8 (21%)	3 (12%)
Graft	Left lobe	31 (50%)	20 (53%)	11 (46%)
	Right lobe	31 (50%)	18 (47%)	13 (54%)
GW/RBW (%)	=0.8	44 (71%)	26 (68%)	18 (75%)
	<0.8	18 (29%)	12 (32%)	6 (25%)
Bile duct orifices in graft	Multiple	14 (22%)	7 (18%)	7 (29%)
	Single	49 (79%)	32 (84%)	17 (71%)
Bile duct reconstruction	D-D	38 (61%)	38 (100%)	0 (0%)
	R-Y	24 (39%)	0 (0%)	24 (100%)
Post-operative complications	Bile leak	13 (21%)	7 (18%)	6 (25%)
	Post-op. bleeding	11 (18%)	5 (13%)	6 (25%)
	Acute cellular rejection	12 (19%)	7 (18%)	5 (21%)
	Biliary stricture	15 (24%)	12 (32%)	3 (12%)

GW/RBW = graft-to-recipient weight ratio, D-D = duct-to-duct hepaticocholedochostomy, R-Y = Roux-en-Y hepaticojejunostomy.

Tab. 2: Technical procedures for biliary reconstruction and biliary tube placement

	–2006.9 ($n=38$)	2006.10– ($n=23$)
Suture	5-0 or 6-0 PDS, interrupted or continuous	Same as left
Peribiliary plexus	Preserved	Same as left
Biliary reconstruction	D-D or R-Y Criteria for selection included number and size of bile duct orifice, tension at the anastomosis, and distance between the orifices in graft	D-D only
Biliary tube		
• Route	(1) Cystic duct to common bile duct of recipient (C-tube) (2) Common bile duct to orifice (T-tube) (3) Common bile duct to orifice or (4) Opposite side of hepatic duct to graft orifice	(5) Common bile duct to orifice
• Tip	Not beyond the anastomosis in route (1) Beyond the anastomosis in route (2) to (4)	Beyond the anastomosis in all cases
• All orifices or not	Not necessarily in all arofices	In all orifices
Removal of the tube	3 months after operation	6 months after operation

Before September 2006, the biliary tube route (1) was applied in the first 10 cases and then one of the routes (2) to (4) was selected in the last 28 cases. Schemes are in cases of right lobe graft.
PDS = polydioxanone suture, D-D = duct-to-duct hepaticocholedochostomy, R-Y = Roux-en-Y hepaticojejunostomy.

confirmed. Stenosis was detected by CT scan, magnetic resonance cholangiography, endoscopic retrograde cholangiography, or percutaneous transphepatic cholangiography.

Surgical procedures before and after September 2006

Surgical procedures for biliary reconstruction and placement of biliary tubes before and after September 2006 are summarized in Table 2. Details of the procedures are as follows.

Between June 1997 and September 2006

We employed both R-Y and D-D. Between June 1997 and January 2002, R-Y was the first choice, but D-D was used when the bile duct orifice was single, the size of the recipient's bile duct seemed to match that of the donor's bile duct, and no tension was applied to the anastomosis. Between February 2002 and September 2006, the criteria for applying D-D was gradually extended, and D-D was used even in cases of multiple duct orifices or when there was a size mismatch between the bile ducts. We did not encounter any grafts with more than 3 bile duct orifices, and all grafts had single or double orifice (s). The double orifices were formed into a single duct, in cases where doing so was feasible, and the newly formed duct was then anastomosed to the recipient's bile duct. R-Y was still used in cases where it was not feasible to form multiple bile duct orifices in a graft into a single duct.

For R-Y, the bile duct was anastomosed to the R-Y limb of the jejunum using 5-0 or 6-0 polydioxanone suture (PDS) in an interrupted or continuous fashion. A biliary tube was routinely used and introduced through the R-Y limb of the jejunum.

For D-D, an end-to-end hepaticocholedochostomy was performed using 5-0 or 6-0 PDS in an interrupted or continuous fashion. In both the recipient and donor operations, careful attention was paid to preserving the vascular plexus around the bile duct. In donor surgery, we avoided dissection of connective tissues around the bile duct and cut the bile duct after dissection of all parenchymal tissue. The bile duct of the recipient was also prepared carefully with minimal dissection so that the blood supply to the bile duct was maintained. As a biliary drainage tube, a C-tube was inserted from the cystic duct to the recipient's common bile duct routinely between June 1997 and January 2002 (route [1] in Table 2). The tip of C-tube was not placed beyond the anastomosis. After January 2002, a biliary tube was inserted from the common bile duct (route [2] and [3] in Table 2) or on the opposite side of the hepatic duct (route [4] in Table 2); this necessitated placing the tip beyond the anastomosis so that the tube served as a stent (schemes are shown in Table 2). When the bile ducts of the graft were double and formed in a single duct, the tube was inserted in 1 of the ducts through the formed anastomosis. The biliary tube was removed 3 months after operation.